

THERMAL STRATIFICATION IN FACTORIES
WITH HIGH CEILINGS

by

RICHARD A. BEIER

B.S., Kansas State University, 1975

A MASTER'S THESIS

submitted in partial fulfillment of the
requirements for the degree

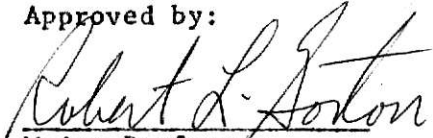
MASTER OF SCIENCE

Department of Mechanical Engineering

KANSAS STATE UNIVERSITY
Manhattan, Kansas

1976

Approved by:


Major Professor

LD
2668
T4
1976
B446
C.2
Document

TABLE OF CONTENTS

| Chapter | Page |
|--|------|
| I. INTRODUCTION | 1 |
| II. PREVIOUS INVESTIGATIONS | 3 |
| III. DETAILED DESCRIPTION OF THE PHYSICAL MODEL | 6 |
| IV. ANALYSIS OF THE STRATIFICATION PROCESS | 13 |
| Thermal Plumes | 13 |
| An Equivalent Virtual Source | 20 |
| Rejection of Ventilation Air Through the Stratified Layer | 25 |
| Transient Energy Equations | 25 |
| The Heat Flow Rates | 32 |
| V. NUMERICAL SOLUTION | 37 |
| Position of the Virtual Source | 37 |
| Finite Difference Procedure | 39 |
| Error Analysis | 40 |
| Thickness of the Stagnant Layer | 42 |
| Procedure of the Computer Program | 42 |
| VI. RESULTS AND DISCUSSION | 44 |
| Comparison with the Plant Data | 45 |
| Varying Parameters in the Model | 54 |
| VII. SUMMARY AND CONCLUSIONS | 62 |
| VIII. RECOMMENDATIONS | 64 |
| LIST OF REFERENCES | 65 |
| APPENDIX | 67 |
| Appendix A | 68 |
| Appendix B | 71 |
| Appendix C | 79 |
| Appendix D | 92 |
| ACKNOWLEDGEMENTS | 95 |
| VITA | 96 |

LIST OF FIGURES

| Figure | | Page |
|--------|---|------|
| 1 | Profile of a Factory in the Physical Model | 7 |
| 2 | Diagram of the Fluid Motion Within the Stratified Layer | 9 |
| 3 | The Fluid Motion if Air is Exhausted Through the Stratified Layer for the Three Possible Cases | 12 |
| 4 | Point Source in a Cylindrical, Confined Region | 16 |
| 5 | Typical Middle Section of a Factory Where the Lighting Effects are Equivalent to a Single Light Fixture | 22 |
| 6 | Vertical Coordinate System for the Middle Section of the Factory | 27 |
| 7 | A Spatial Element of the Surrounding Air in the Plume Layer | 29 |
| 8 | Direction of Heat Flow Rates | 33 |
| 9 | Comparison of Numerical Results with Plant Data for the Total Cooling Load | 47 |
| 10 | Thickness of the Stagnant Layer For Different Values of T_m | 48 |
| 11 | Comparison of Numerical Results with Plant Data for the Temperature Profiles | 49 |
| 12 | Instantaneous Heat Flow Rates for the Roof and the Stratified Layer | 51 |
| 13 | Instantaneous Heat Flow Rates for the Cooled Space and the Floor | 52 |
| 14 | Cumulative Thermal Storage of the Roof, Floor and Stratified Layer | 53 |
| 15 | Effect of Varying the Light Load on the Peak Cooling Load | 55 |
| 16 | Effects of Varying the Thickness of Roof Insulation | 59 |
| 17 | Comparison of the Peak Cooling Load With and Without Exhausting Ventilation Air through the Stratified Layer | 60 |

| Figure | | Page |
|--------|--|------|
| 18 | Sufficient Air Flows Exhausted through the Stratified Layer which Reduce the Cooling Load by the Convective Portion of the Lighting Load | 61 |
| 19 | Arrangement of Finite Difference Nodes | 72 |

LIST OF TABLES

| Table | | Page |
|-------|--|------|
| 1 | Energy Rates on a Spatial Element of the Surrounding of the Plume Layer | 28 |
| 2 | Description and Thickness of Nodes | 75 |

NOMENCLATURE

| Symbol | Significance | Units |
|------------|--|--|
| A_f | Floor area of factory | ft^2 |
| A_w | Area of Exterior Walls of factory | ft^2 |
| b | Characteristic horizontal scale of the normal distribution curve | ft |
| c_a | Specific heat of air at constant pressure | $\text{Btu/lbm-}^\circ\text{F}$ |
| c_f | Specific heat of the floor material | $\text{Btu/lbm-}^\circ\text{F}$ |
| c_{st} | Specific heat of roof supporting steel | $\text{Btu/lbm-}^\circ\text{F}$ |
| c_1 | Specific heat of ceiling material | $\text{Btu/lbm-}^\circ\text{F}$ |
| c_2 | Specific heat of middle roof material | $\text{Btu/lbm-}^\circ\text{F}$ |
| c_3 | Specific heat of top roof material | $\text{Btu/lbm-}^\circ\text{F}$ |
| C_g | Thermal conductance of earth between the floor and the ground of constant temperature | $\text{Btu/hr-ft}^2\text{-}^\circ\text{F}$ |
| CC | Constant denominator in the nodal equations containing the thermal storage of structural steel | $\text{Btu/}^\circ\text{F}$ |
| d_s | Distance between virtual and actual plume sources | ft |
| d_s^u | Notation to indicate the u iteration of d_s | ft |
| d_{lc} | Vertical distance between light fixtures and the ceiling | ft |
| E_{flst} | Cumulative thermal storage of the floor per unit area | Btu/ft^2 |
| E_{rst} | Cumulative thermal storage of the roof per unit area | Btu/ft^2 |
| E_{sst} | Cumulative thermal storage of the stratified layer per unit area | Btu/ft^2 |

| Symbol | Significance | Units |
|----------|--|---|
| f | Dimensionless, axial density deficiency in the plume | dimensionless |
| f_o | Dimensionless density deficiency of the environment of the plume | dimensionless |
| F_o | Buoyancy flux of a point source relative to some chosen density | ft^4/sec^3 |
| F_{as} | Buoyancy flux of an actual source relative to some chosen density | ft^4/sec^3 |
| F_{rl} | Fraction of power output of light fixtures that is dissipated by radiation to the floor | dimensionless |
| F_{st} | Fraction of nodal volume occupied by supporting steel of the roof | dimensionless |
| g | Gravitational acceleration | ft/sec^2 |
| g_c | Gravitational constant | $\text{lbm}\cdot\text{ft}/\text{lbf}\cdot\text{sec}^2$ |
| h | Dimensionless horizontal scale of the plume width | dimensionless |
| h_c | Convective heat transfer coefficient for the ceiling surface and the air of the stratified layer | $\text{Btu}/\text{hr}\cdot\text{ft}^2\cdot^{\circ}\text{F}$ |
| h_f | Convective heat transfer coefficient for the floor surface and the air of the cooled space | $\text{Btu}/\text{hr}\cdot\text{ft}^2\cdot^{\circ}\text{F}$ |
| h_r | Radiation heat transfer coefficient for the surfaces of the ceiling and floor | $\text{Btu}/\text{hr}\cdot\text{ft}^2\cdot^{\circ}\text{F}$ |
| h_s | Coefficient of heat transfer by radiation and convection at the outer roof surface | $\text{Btu}/\text{hr}\cdot\text{ft}^2\cdot^{\circ}\text{F}$ |
| H | Height of an enclosed region containing the plume | ft |
| i | Integer used in numbering nodal equations and boundaries | dimensionless |
| j | Dimensionless velocity of the surrounding air of the plume | dimensionless |
| k | Dimensionless product of the axial, vertical velocity and horizontal scale of the plume | dimensionless |

| Symbol | Significance | Units |
|------------------|--|-------------------------|
| k_a | Thermal conductivity of air | Btu/hr-ft- $^{\circ}$ F |
| k_f | Thermal conductivity of the floor material | Btu/hr-ft- $^{\circ}$ F |
| k_r | Thermal conductivity of the homogenous roof material | Btu/hr-ft- $^{\circ}$ F |
| k_1 | Thermal conductivity of the bottom roof material | Btu/hr-ft- $^{\circ}$ F |
| k_2 | Thermal conductivity of the middle roof material | Btu/hr-ft- $^{\circ}$ F |
| k_3 | Thermal conductivity of the top roof material | Btu/hr-ft- $^{\circ}$ F |
| z | Dimensionless axial, vertical velocity of the plume | dimensionless |
| L_1 | Height of the floor lower surface | ft |
| L_2 | Height of the light level | ft |
| L_3 | Height of the boundary between the plume and stagnant layers | ft |
| L_4 | Height of the ceiling or inner roof surface | ft |
| L_5 | Height of the outer roof surface | ft |
| \dot{m}_{al} | Mass flow rate from the air conditioned space into a plume | lbm/sec |
| \dot{m}_d^i | Downward mass flow rate of the surrounding air across the i th nodal boundary per unit area | lbm/sec-ft 2 |
| \dot{m}_u^i | Upward mass flow rate of the surrounding air across the i th nodal boundary per unit area | lbm/sec-ft 2 |
| \dot{m}_{pl}^i | Mass flow rate of the surrounding air without superposition of any ventilation air flow across the i th nodal boundary per unit area | lbm/sec-ft 2 |
| N | Total number of nodes | dimensionless |
| q_{cd} | Conduction energy rate for spatial element of the surrounding air | Btu/hr-ft 2 |
| q_{cv} | Convective energy rate for spatial element of the surrounding air | Btu/hr-ft 2 |
| q_{hl} | Total power output of lights per unit floor area | Btu/hr-ft 2 |

| Symbol | Significance | Units |
|-----------------|---|------------------------|
| q_{st} | Internal storage energy rate for spatial element of the surrounding air | Btu/hr-ft ² |
| q_{sb} | Heat flow rate from the stratified layer to the air conditioned space per unit floor area | Btu/hr-ft ² |
| q_{acb} | Heat flow rate into the cooled space from the stratified layer and outdoor ventilation air flow per unit floor area | Btu/hr-ft ² |
| q_{acl} | Cooling rate supplied by the air conditioning system per unit floor area | Btu/hr-ft ² |
| q_{cvp} | Convective energy rate for the spatial element of the surrounding air | Btu/hr-ft ² |
| q_{rad} | Radiant heat flow rate from the ceiling to the floor surface per unit area | Btu/hr-ft ² |
| q_{rst} | Instantaneous thermal storage rate of the roof per unit area | Btu/hr-ft ² |
| q_{sst} | Instantaneous thermal storage rate of the stratified layer per unit area | Btu/hr-ft ² |
| q_{ceil} | Convective heat flow rate from the ceiling to the stratified layer per unit area | Btu/hr-ft ² |
| q_{flin} | Convective heat flow rate from the floor to the cooled space per unit area | Btu/hr-ft ² |
| q_{flst} | Instantaneous thermal storage rate of the floor per unit area | Btu/hr-ft ² |
| q_{roof} | Heat flow rate into the roof by radiation and convection at the outer roof surface per unit area | Btu/hr-ft ² |
| q_{check} | Approximation of the roundoff error by checking the heat flow rates in an energy balance for the overall system | Btu/hr-ft ² |
| q_{flout} | Conduction heat flow rate from the bottom floor surface into the ground per unit area | Btu/hr-ft ² |
| \bar{q}_{int} | Internal energy generation within the air conditioned space | Tons of refrigeration |
| \bar{q}_{tot} | Total air conditioning load for the factory | Tons of refrigeration |

| Symbol | Significance | Units |
|------------------|--|--------------------------------------|
| \bar{q}_{wall} | Heat transfer rate through the exterior walls | Tons of refrigeration |
| q_{acb}^p | Heat flow rate into the cooled space from the stratified layer and outdoor ventilation air flow per unit area at time of peak cooling load | Btu/hr-ft ² |
| q_{acl}^p | Peak cooling rate supplied by the air conditioning system per unit floor area | Btu/hr-ft ² |
| q_{fln}^p | Convective heat flow rate from the floor to the cooled space per unit area at time of peak cooling load | Btu/hr-ft ² |
| Q_v | Ventilation air flow rate per unit area | ft ³ /min-ft ² |
| Q_{hl} | Total power output of a single light fixture | Btu/hr |
| Q_{sl} | Total power output of a single light fixture | Btu/sec |
| r | Radial coordinate measured from the axis of the plume | ft |
| r_e | Effective plume radius ($r_e = 2.146b$) | ft |
| r_p | Radius of a plume where the velocity and density are constant across it | ft |
| R | Radius of a cylindrical region | ft |
| S | Thickness of the plume layer | ft |
| t | Time | sec or hr |
| Δt | Time increment | hr |
| T_b | Bulk temperature of the plume at the light level | °F |
| T_f | Temperature in the floor | °F |
| T_g | Ground temperature | °F |
| T_m | Maximum or axial temperature in the plume at the light level | °F |
| T_o | Temperature in the surrounding air of the plume | °F |
| T_p | Temperature in the plume | °F |

| Symbol | Significance | Units |
|-------------|---|--------------------------------------|
| T_{ac} | Desired temperature of the air conditioned space | $^{\circ}F$ |
| T_{oa} | Temperature of the outside air | $^{\circ}F$ |
| T_{pl} | Temperature in the plume layer of the surrounding air | $^{\circ}F$ |
| T_{sl} | Temperature in the stagnant layer | $^{\circ}F$ |
| T_{aac} | Desired, absolute temperature of the air conditioned space | $^{\circ}R$ |
| T_{acc} | Temperature of the lower space when air conditioning system is off | $^{\circ}F$ |
| T_{oal} | Temperature of the surrounding air at the light level | $^{\circ}F$ |
| T_{sat} | Sol-air temperature | |
| T_n^t | Temperature of nth node at time t | $^{\circ}F$ |
| T_n^{t+1} | Temperature of nth node at time $t+\Delta t$ | $^{\circ}F$ |
| U_{pl} | Velocity of the surrounding air in the plume layer | ft/hr |
| U_{sl} | Velocity of the air in the stagnant layer | ft/hr |
| U_w | Overall heat transfer coefficient of exterior walls | Btu/hr-ft ² - $^{\circ}F$ |
| U_h | Velocity of the surrounding air due to the plume motion | ft/hr |
| U_s | Velocity of the surrounding air due to the plume motion | ft/sec |
| U_{al} | Downward velocity of the surrounding air due to the plume motion at the light level | ft/sec |
| v | Horizontal velocity in the surrounding air due to entrainment | ft/hr |
| V | Upward velocity of ventilation air exhausted through the stratified layer | ft/sec |
| w | Axial velocity in the plume | ft/sec |
| \bar{w} | Velocity in the plume | ft/sec |

| Symbol | Significance | Units |
|------------|--|---------------------------|
| ΔW | Change of humidity ratio for ventilation air flow | lbm water/ lbm dry air |
| y | Coordinate measured vertically upward from bottom surface of floor | ft |
| y_f | Spatial increment of the floor nodes | ft |
| y_s | Spatial increment of the nodes in the stratified layer | ft |
| y_{ac} | Thickness of air conditioned space | ft |
| y_1 | Spatial increment of lower roof node | ft |
| y_2 | Spatial increment of middle roof nodes | ft |
| y_3 | Spatial increment of top roof node | ft |
| z | Coordinate measured vertically upward from a point plume source | ft |

Greek Letters

| | | |
|----------------|---|---------------------|
| α | Entrainment constant | dimensionless |
| α_a | Thermal diffusivity of air | ft ² /hr |
| α_f | Thermal diffusivity of floor material | ft ² /hr |
| α_r | Thermal diffusivity of roof material | ft ² /hr |
| β | Coefficient of thermal expansion | 1/ ^o R |
| Δ | Axial density deficiency in the plume | ft/sec ² |
| Δ_0 | Density deficiency in the surrounding air | ft/sec ² |
| $\bar{\Delta}$ | Density deficiency in the plume | ft/sec ² |
| ϵ_c | Radiant emissivity of the ceiling | dimensionless |
| ϵ_f | Radiant emissivity of the roof | dimensionless |
| ξ | Dimensionless height of the plume | dimensionless |
| ξ_s | Dimensionless height of a actual source | dimensionless |

| Symbol | Significance | Units |
|-------------|---|---------------------|
| ξ^i | Dimensionless height of the i th nodal boundary | dimensionless |
| θ | Angle in cylindrical coordinate system | dimensionless |
| ρ_a | Density of air | lbm/ft ³ |
| ρ_f | Density of floor material | lbm/ft ³ |
| ρ_o | Density of the surrounding air | lbm/ft ³ |
| ρ_p | Density in the plume | lbm/ft ³ |
| ρ_r | Reference density | lbm/ft ³ |
| ρ_{st} | Density of the structural steel | lbm/ft ³ |
| ρ_1 | Density of bottom roof node | lbm/ft ³ |
| ρ_2 | Density of middle roof nodes | lbm/ft ³ |
| ρ_3 | Density of top roof node | lbm/ft ³ |

CHAPTER I

INTRODUCTION

Concern for the health and comfort of the factory worker by union and government officials and by management has stimulated a growing interest in the air conditioning of factories. In recent years designers of industrial air conditioning systems have taken advantage of thermal stratification, and significant savings have been achieved by cooling only the lower, occupied levels of spaces with high ceilings (1-4)*.

The warmer air near concentrated heat sources such as lights or machinery tends to rise to the ceiling due to its buoyancy. Thus, part of the internal heat generated is removed from the air conditioned space. Also, a large part of the usual roof load does not enter the lower level since it is blocked by warmer air near the ceiling. This causes the air near the ceiling to be formed into horizontal layers having different temperatures. Such an arrangement is called a stratified layer.

A lack of design information about stratification in high ceiling plants sometimes leads to poor agreement between the calculated and actual air conditioning load (4). Also, designers disagree about the effects of air being exhausted through the stratified layer. Dralle (3) favors ventilation of upper levels while Dean (1) thinks the air above the lower conditioned level should be kept as motionless as possible. The required

*Number in parenthesis designate references in the List of References.

height for stratification to occur and the possible advantages of increased ceiling height have not been examined. A method to predict the air circulation in a stratified layer due to internal loads, ventilation systems and the time dependent boundary condition at the roof is desired. The purpose of this work is to provide an adequate theoretical analysis of the problem and obtain some needed design information. The investigation is restricted by considering the light fixtures as the only internal sources which affect the stratification process.

The phenomenon of thermal stratification is not limited to the present situation. For example, the yearly variation in solar heating of lakes creates a time dependent vertical temperature distribution. Also, the stratification of cryogenic fluids in supply tanks is important when these fluids are used as rocket propellants.

In the present investigation a physical model of a typical section in the middle of a factory was considered. With the aid of previous analytical and laboratory studies of stratification and natural convection the energy equations were written. The time dependent boundary condition and the simultaneous modes of heat transfer complicate the problem and prevent an exact solution of the equations. The appropriate implicit finite difference equations were written and solved by Gauss-Jordan elimination. A Fortran computer program was written and a numerical solution for the daily cycle was obtained.

Actual data taken from a factory with an air conditioning system designed for thermal stratification provided a verification of the solution. By varying parameters in the model a number of interesting solutions were obtained which include the effects of exhausting ventilation air through the stratified layer and the result with increased ceiling height.

CHAPTER II

PREVIOUS INVESTIGATIONS

Significant reductions in the required air conditioning capacity of factories due to thermal stratification have been reported by Dean (2), Dralle (3) and Olivieri (4). Data including the transient air conditioning load from an operating day at a plant in Kansas City, Missouri was obtained by Dean (2). The case study provided by Dean was compared to the numerical solution of this study.

Most of the previous theoretical work concerning stratification phenomena concentrated on very specific conditions, which is typical of the available solutions regarding any natural convection problem. Stratification occurrences have been studied in several different applications, including the natural happenings in the atmosphere and large bodies of water. Despite the lack of theoretical work concerning stratification in high ceiling plants, the following references provided some insight.

A theory of turbulent natural convection from maintained and instantaneous sources was presented by Morton, Taylor and Turner (5). Solutions in both uniform and linearly stratified environments were obtained. The plumes of hot air rising from small sources were treated as conical in shape as observed in experiments. The rate of entrainment of surrounding fluid at any height was assumed to be proportional to a characteristic velocity at that height. Results of previous and new experiments were compared with the theory which showed good agreement. An application of the theory to the

atmosphere was made.

Baines and Turner (6) considered turbulent plumes in a bounded region where interaction between the buoyant elements and the environment exists. A steady-state solution produces a stably stratified environment with the density profile fixed in shape. In addition to the entrainment assumption of Morton et al (5), they regarded the rising elements as spreading out at the top of the region and becoming part of the environment at that level. Laboratory experiments verify the results of the theory. In the present study a plume of hot air rising from each light fixture was assumed to be of this form.

The various conditions, including stratified environments, under which solutions for buoyant elements from maintained and instantaneous sources have been obtained were reviewed by Turner (7).

An analytical and experimental study of natural convection in cylindrical coordinates was presented by Barakat and Clark (8). Interest in thermal stratification in liquid propellant tanks where the container walls are heated motivated the work. The governing equations were solved numerically and their method offers some guidance in the numerical solution of non-linear partial differential equations.

Winter and Schoenhals (9) also investigated stratification of a contained fluid subject to transient heat convection from the container sides. As in the present study, a stratified layer which forms at the top of the container is fed by rising hot air. An analytical solution based on an approximate integral method was obtained. Also, results of several experiments concerning the behavior of the stratification process were presented and possible methods to prevent it were obtained.

Like the roof of a factory, a large body of water receives periodic, solar heating. An analytical method for the prediction of the time dependent vertical temperature distribution in a deep lake was presented by Dake and Harleman (10). Their theory for the yearly cycle of solar heating and cooling agreed well with field data. Armaly and Lepper (11) obtained a numerical solution for the daily stratification process in deep bodies of water by taking into account the directional and spectral behavior of the solar load.

CHAPTER III

DETAILED DESCRIPTION OF THE PHYSICAL MODEL

The first step toward simulating an occurrence in nature is the production of a qualitative description of the phenomenon. From the previous investigations of thermal stratification and the physical structure of an industrial plant, a model which includes the various mechanisms of heat transfer was developed. The following discussion of the physical model provides an introduction to the basic ideas of stratification in high ceiling plants.

This investigation was restricted by considering the light fixtures as the only internal load which affects the stratification process. The effects of turbulence in the cooled space on rising, warmer air from a concentrated source on the floor includes some removal of fluid from the rising currents by the environment. Since the level of turbulence may depend on numerous conditions within the cooled space, this complication was not considered in this study. Thus, discrete, large heat sources at the floor were not examined and a uniformly distributed source around the floor was assumed to be part of the air conditioning load.

In the model the lights separate the air conditioned space below and the warmer stratified air above, as shown in Figure 1. Proper placement of the supply air diffusers and the return air inlets sufficiently below the light fixtures eliminates the interference of their air flow with the stratified layer. In the actual case there exists an air space between the cooled space and the light fixtures but it provides negligible thermal storage. Since only overall effects of air movements are important the

**THIS BOOK
CONTAINS
NUMEROUS PAGES
WITH DIAGRAMS
THAT ARE CROOKED
COMPARED TO THE
REST OF THE
INFORMATION ON
THE PAGE.**

**THIS IS AS
RECEIVED FROM
CUSTOMER.**

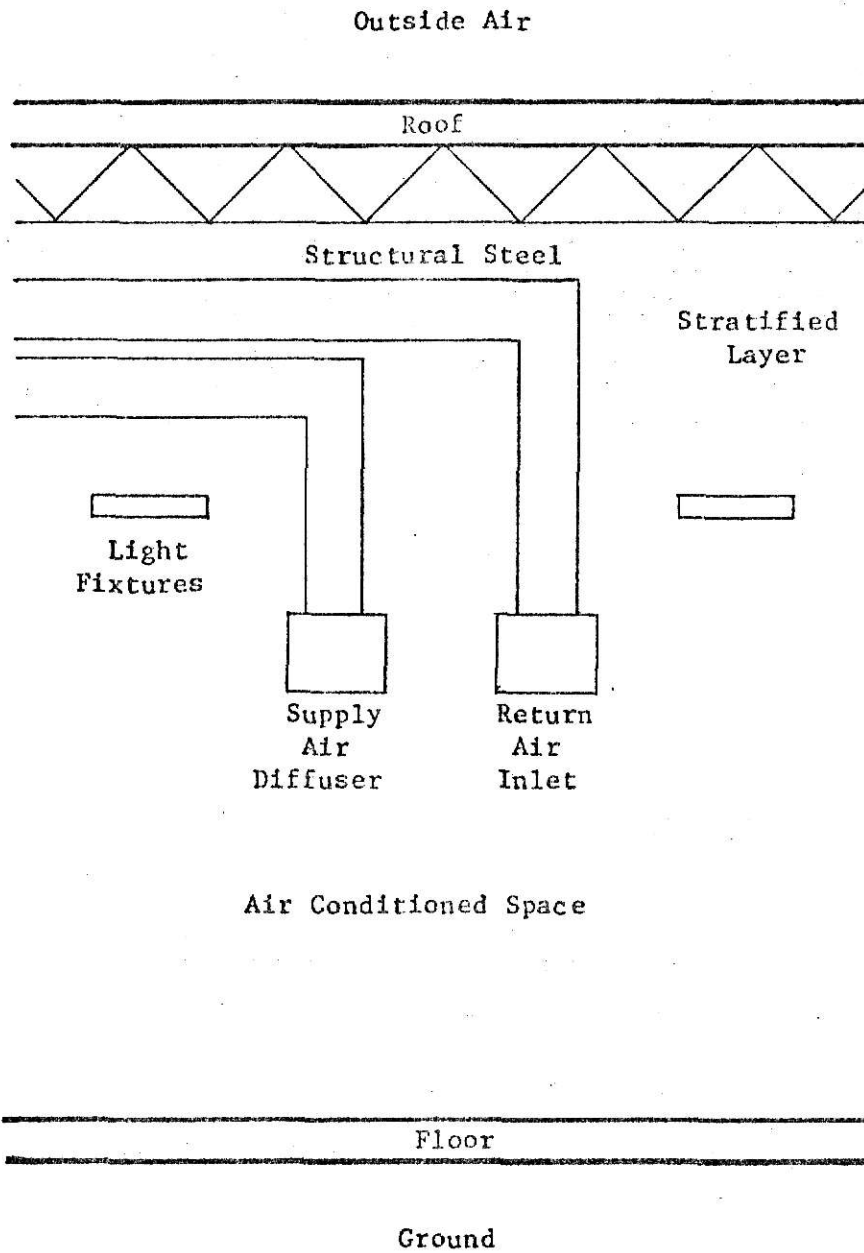


Figure 1. Profile of a Factory in the Physical Model

imaginary boundary defined by the light fixtures provides an adequate approximation. Also, it was assumed that sufficient fluid motion exists in the cooled space to provide a constant uniform temperature.

The boundary condition at the outside of the roof varies with time in a 24 hour cycle. The heat balance at this boundary at any set time includes solar radiation, radiant heat transfer with the sky and other outside surroundings and convection heat transfer with the outside air. Radiant heat exchange occurs between the ceiling and the floor and convection heat transfer takes place between the ceiling and the top air of the stratified layer. Between the floor and the air conditioned space convection exists and conduction occurs between the floor and the ground. The ground acts as an infinite heat sink since below a certain depth its temperature remains unchanged. The thermal storage of the roof, the roof supporting steel and the floor is significant.

Consider a circular region in the middle of the factory of appropriate size so that a single light fixture can supply it with light. Of course in the actual case the light supplied by different fixtures overlaps and no such boundaries are observed. Each light fixture generates sensible heat which is dissipated by radiation to the floor surface and convection to the surrounding air. As the neighboring air becomes heated it rises, since its density decreases, and it is replaced by new air from the air conditioned space. The rising turbulent plume grows in mass as it entrains air at its edge from the non-turbulent environment. Figure 2 shows the fluid motion within the stratified layer and the arrows indicate the direction of flow. The heated air continues upward until it reaches the ceiling where it spreads out uniformly and becomes part of the environment. Previously affected

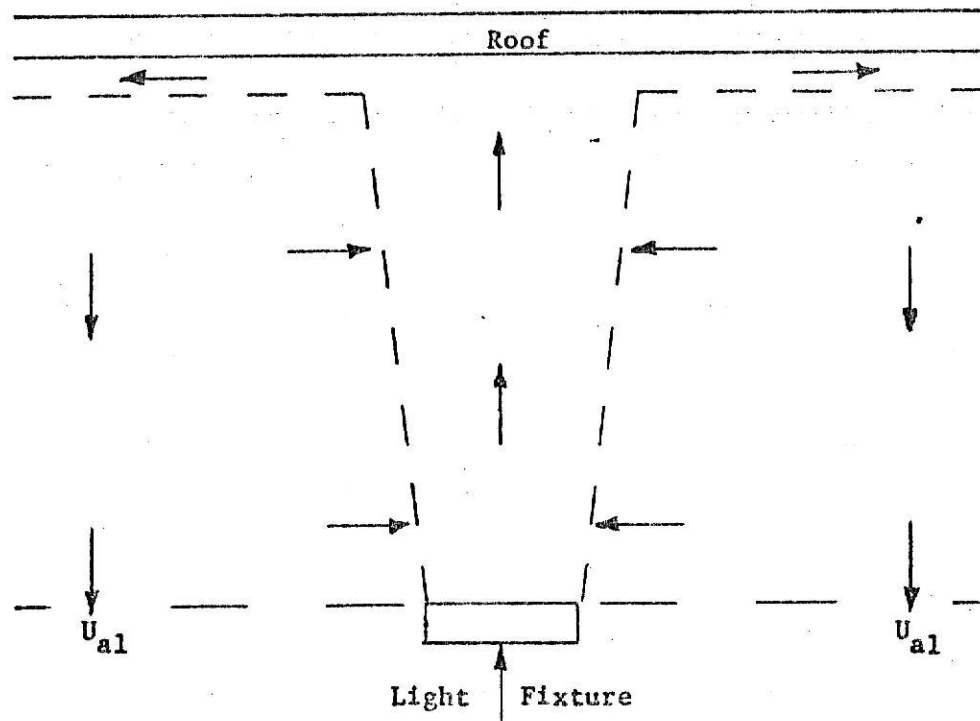


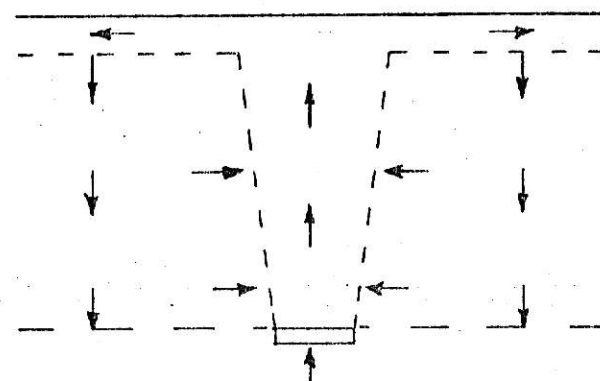
Figure 2. Diagram of the Fluid Motion within the Stratified Layer

layers are continuously pushed downward until they reach the air conditioned space below.

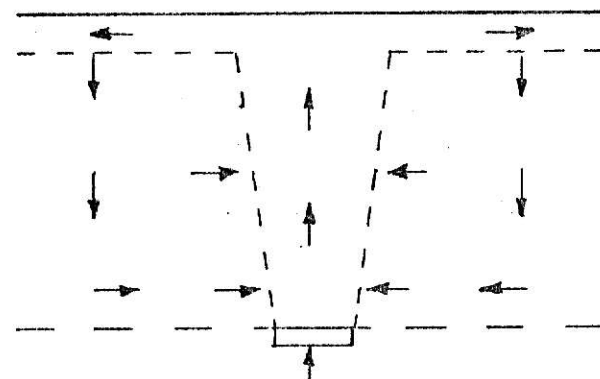
The upper air of the stratified layer also receives heat by convection from the ceiling. Consider the case when the ceiling heat flow is sufficient to raise the neighboring air temperature higher than the average temperature of the rising convection currents at that height. The rising plume does not penetrate this warmer layer which remains stagnant despite the fluid motion below. The identical effects on the convection currents below could be created by lowering the ceiling at a height equal to the thickness of the stagnant layer. A virtual ceiling at the boundary of the stagnant layer and the plume layer is seen by the rising currents and the same type of fluid motion as described previously exists below the stagnant layer.

Sometimes needed ventilation air for the cooled space is exhausted through the stratified layer and out at the roof. It was assumed that this does not alter the motion within the plume and the entrainment at any level remains unchanged. These assumptions follow if the exhaust fans are not placed directly over the rising plumes but they are located above the surrounding air which is under most of the ceiling area. Note that in the previous situations the same amount of air drawn by the light fixture into the rising currents must be returned to the air conditioned space through the surrounding air. Therefore, three possibilities exist for a given ventilation rate superimposed on the fluid motion of the surrounding air of a given plume. The upward ventilation velocity may be less than, equal, or greater than the undisturbed downward velocity of the surrounding air at the light level. Figures 3a, b and c show the changed fluid motion corresponding to the three different cases. Also, a stagnant layer relative to the plume, as described

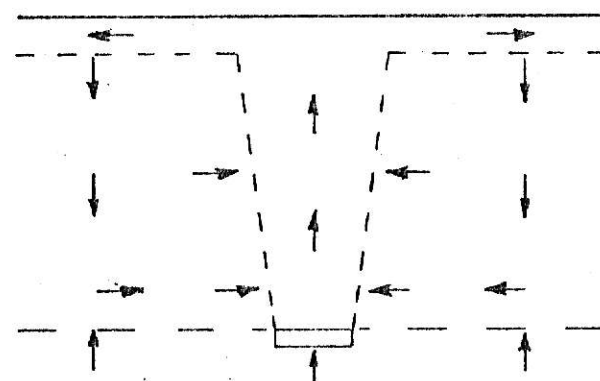
previously, could exist where the fluid motion within the layer is the uniform ventilation velocity.



a) $V < U_{a1}$



b) $V = U_{a1}$



c) $V > U_{a1}$

Figure 3. The Fluid Motion if Air is Exhausted Through the Stratified Layer for the Three Possible Cases

CHAPTER IV

ANALYSIS OF THE STRATIFICATION PROCESS

Consider a typical circular section in the middle of the factory where the total lighting effects on the floor are equivalent to those produced by a single light fixture. The time varying boundary condition at the roof and the multiple modes of heat transfer within the plant hinder the derivation of exact solution. Therefore, the objective of this analysis was to develop a mathematical statement of the stratification process which could be solved by numerical methods.

The first portion of the analysis involved the steady-state equations which describe the thermal plume phenomena. Then, the equations representing replacement of a light fixture with an equivalent virtual source were obtained. The derivation of the energy equation for the air surrounding the plume and the statement of the energy equations for the floor and ceiling with appropriate boundary conditions followed. Finally, the heat flow equations including all the different modes of heat transfer within the space were listed.

Thermal Plumes

Turbulent plumes of hot air rising from small sources tend to be confined within conical regions similarly to the case of forced jets as noted by Turner (7). An observable boundary between the turbulent buoyant fluid and the surroundings has been noted from laboratory experiments. The turbulent plume grows with distance upward as some of the non-turbulent

external fluid flows into it.

Morton et al (5) considered a source of buoyancy as a general case of natural convection. The results may be applied to a source of light liquid in a heavier liquid with which it is freely miscible or to the more obvious case of a source of heat in a fluid. His results and others have been given with density as one of the dependent variables defining the convective motion. To transfer density into terms of temperature the relation

$$\frac{\rho_o - \rho_p}{\rho_r} = \beta(T_p - T_o) \quad (1)$$

may be used. ($\beta = 1/T$, $^{\circ}R^{-1}$, for gases.) The strength of a source of buoyancy is the total rate of release of buoyancy to the nearby fluid relative to some chosen density. A point source is usually chosen since it is easiest to handle mathematically.

Three main assumptions are common in the discussions of thermal plumes found in the literature. First, the rate of entrainment at the edge of the plume is proportional to the mean velocity in the plume at that height. Although this is done without an understanding of the details of the turbulent mixing, experiments have verified this assumption. Second, the velocity and the buoyancy profiles are of Gaussian form and are equal in width. The profiles may be expressed as

$$\bar{w}(z,r) = w(z) \exp(-r^2/b^2) \quad (2)$$

$$\bar{\Delta}(z,r) = \frac{(\rho_o(z) - \rho_p(z,r))}{\rho_r} = \Delta(z) \exp(-r^2/b^2) \quad (3)$$

The horizontal scale b is characteristic of the normal distribution curve and does not correspond to the radius of the plume. However, $r_e = 2.146b$ is an effective radius where the velocity and density difference have decreased to

1% of the axial values. Third, the local density variations of any height are small compared to the chosen reference density.

A point source of buoyancy in an enclosed space was considered by Baines and Turner (6), in which changes in the environment occur due to the source. The process in a cylindrical container was treated as shown in Figure 4, where again the arrows indicate the directions of flow. It was assumed that when the plume fluid reaches the top of the container it spreads out instantaneously into a thin horizontal layer. After a period of time the entire fluid in the environment has at some time been in the plume. A stable density distribution in the surroundings develops with a continuous decrease in density at any level.

It was assumed that the area containing the plume is a small fraction of the total area at any level and that the velocities in the plume are much larger than those in the environment. Under these additional conditions Baines and Turner (6) wrote the equations of conservation of volume (mass), momentum and density deficiency (the equivalent of thermal energy) as

$$\frac{d}{dz} (b^2 w) = 2\alpha b w \quad (4)$$

$$\frac{d}{dz} \left(\frac{b^2 w}{2} \right) = b^2 \Delta \quad (5)$$

$$\frac{d}{dz} \left(\frac{b^2 w \Delta}{2} \right) = b^2 w \frac{\partial \Delta_0}{\partial z} \quad (6)$$

The entrainment constant, α , must be determined from experimentation. In the last term of equation (6) the density gradient of the surroundings is defined as

$$\Delta_0 = g \frac{\rho_0 - \rho_r}{\rho_r} \quad (7)$$

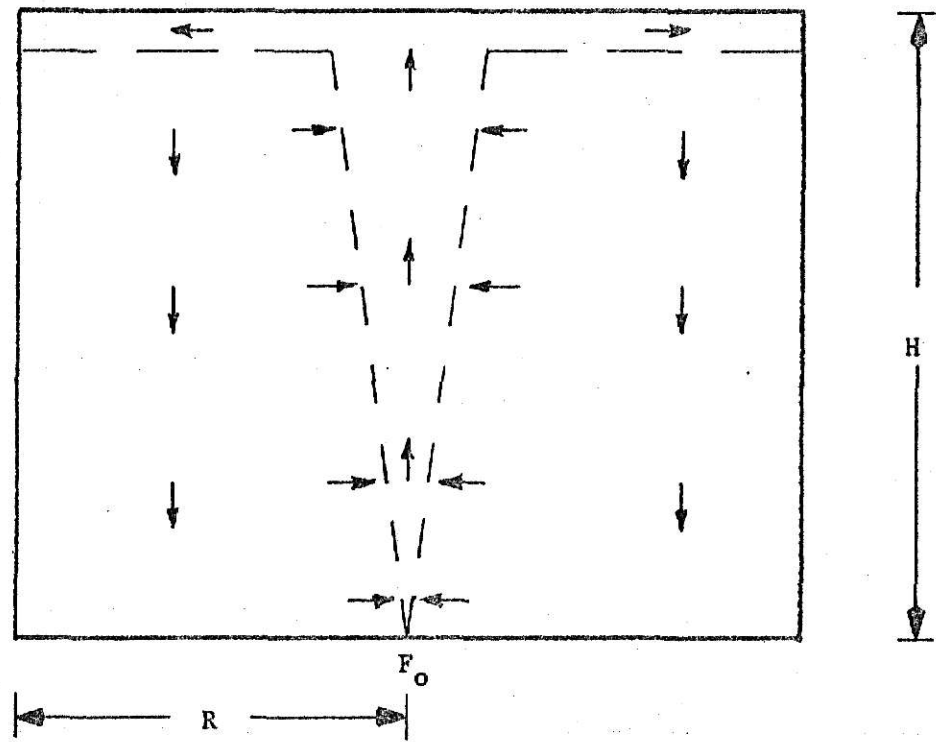


Figure 4. Point Source in A Cylindrical, Confined Region

$$\frac{\partial \Delta_o}{\partial z} = \frac{g}{\rho_r} \frac{\partial \rho_o}{\partial z} \quad . \quad (8)$$

Noting that the downward mass flow in the surroundings at any level equals the upward flow in the plume gave

$$-\pi R U = \pi b^2 w \quad . \quad (9)$$

The fact that the density changes in the surroundings are caused only by the vertical fluid motions was expressed by

$$\frac{\partial \Delta_o}{\partial t} = -U \frac{\partial \Delta_o}{\partial z} \quad . \quad (10)$$

An exact solution was obtained by Morton et al (5) of equations (4), (5) and (6) for the case of a uniform environment. This solution applies only for the rate of advance of the first front of buoyant fluid of the plume in an enclosed region. However, the solution was used later in this analysis for obtaining an approximate virtual source. For boundary conditions it was assumed that at the point source the radius and the momentum in the plume are zero, and that the issue of buoyancy is at a known constant rate. The solution was expressed in terms of powers of z and the constant buoyancy flux as

$$F_o = \frac{1}{2} \pi b^2 w \Delta \Big|_{z=0} \quad (11)$$

$$b(z) = \frac{6}{5} \alpha z \quad (12)$$

$$w(z) = \frac{5}{6\alpha} \left(\frac{18}{5\pi} \alpha F_o \right)^{1/3} z^{-1/3} \quad (13)$$

$$\Delta(z) = \frac{5}{3\pi} \left(\frac{5\pi}{18} \right)^{1/3} \alpha^{-4/3} F_o^{2/3} z^{-5/3} \quad . \quad (14)$$

A brief explanation of the meaning and the units of the buoyancy flux relative to the chosen density may be helpful. By definition

$$F_o = \frac{\text{flux of buoyancy per second from the source}}{\rho_r}$$

Putting the corresponding units in place of the quantities in equation (11) yields

$$F_o \sim \frac{(\text{ft}^2) (\text{ft}/\text{sec}) (\text{ft}/\text{sec}^2) (\text{lbm}/\text{ft}^3)}{\text{lbm}/\text{ft}^3}$$

$$\sim \frac{(\text{lbm} - \text{ft}/\text{sec}^2) / \text{sec}}{\text{lbm}/\text{ft}^3} = \frac{\text{ft}^4}{\text{sec}^3}$$

Dividing both sides of (11) by g_c gives

$$\frac{F_o}{g_c} \sim \frac{(\text{lbm} - \text{ft}/\text{sec}^2) / \text{sec}}{\left(\frac{\text{lbm} - \text{ft}}{\text{lbm} - \text{sec}^2} \right) \frac{\text{lbm}}{\text{ft}^3}} = \frac{\text{lbm}/\text{ft}^3}{\text{lbm}/\text{ft}^3} \quad (15)$$

The numerator of the expression on the right hand side of (15) corresponds to the buoyancy issued by the source and the denominator represents the chosen reference density.

A solution for the full set of equations (4), (5), (6), (9) and (10) was presented by Baines and Turner (6) which is valid after a period of time has elapsed. The variables were expressed in terms of the non-dimensional parameters γ and ξ defined by

$$\xi = \frac{z}{H} \text{ and } \tau = \frac{4}{\pi^{1/3}} \alpha^{4/3} \left(\frac{H}{R} \right)^2 \frac{F_o^{1/3}}{H^{4/3}} t \quad (16)$$

Consider the following transformations which are corrections to those listed by Baines and Turner which appear to be in error:

$$\Delta_o = \frac{\pi^{-2/3}}{4} F_o^{2/3} \alpha^{-4/3} H^{-5/3} (f_o(\xi) - \tau) \quad (17)$$

$$\Delta = \frac{\pi}{2} F_0^{2/3} \alpha^{-4/3} H^{-5/3} f(\xi) \quad (18)$$

$$w = \pi^{-1/3} F_0^{1/3} \alpha^{-2/3} H^{-1/3} l(\xi) \quad (19)$$

$$b = 2 \alpha H h(\xi) \quad (20)$$

$$U_s = 4\pi^{-1/3} F_0^{1/3} \alpha^{4/5} H^{-1/3} (H/R)^2 j(\xi) \quad (21)$$

After defining $k = lh$, substitution of (17)–(21) into (4), (5), (6), (9) and (10) gave

$$\frac{dj}{d\xi} = -k \quad (22)$$

$$\frac{d k^2}{d\xi} = h^2 f \quad (23)$$

$$\frac{d(fj)}{d\xi} = j \frac{df_0}{d\xi} \quad (24)$$

$$j = -lh^2 \quad (25)$$

$$j \left(\frac{df_0}{d\xi} \right) = 1 \quad (26)$$

The boundary conditions applied were

$$f_j = 0 \quad \text{at} \quad \xi = 1 \quad (27)$$

$$j = 0, k = 0, f_0 = 0 \quad \text{at} \quad \xi = 0$$

Baines and Turner obtained a series solution which quickly converges and it was written as

$$-j = lh^2 = 0.459 \xi^{5/3} - 0.0588 \xi^{8/3} - 0.0100 \xi^{11/3} \quad (28)$$

$$k = \lambda h = 0.765 \xi^{2/3} - 0.157 \xi^{5/3} - 0.0366 \xi^{8/3} \quad (29)$$

$$f_j = - (1 - \xi) \quad (30)$$

$$f_o = \xi^{-2/3} (3.27 - 0.837 \xi - 0.062 \xi^2) - 2.37 \quad (31)$$

Laboratory experiments with plumes in an enclosed region verified the solution and the basic assumptions used. The time required for the steady-state solution to be valid is less than a few minutes from the results of the experiments.

The validity of the results obtained with the assumption that the buoyant elements instantaneously spread uniformly across the top of the region is questionable in relatively tall regions. If the inertial force of the rising plume at the top of the region overcomes the restraining buoyancy force, a general overturning motion develops. Baines and Turner related this limitation of their solution with the ratio H/R . In some simple experiments they observed that the thickness of the top layer with overturning motion steadily increased as the ratio H/R was increased. For $H/R = 1.5$ the zone from $\xi = 0.5$ to $\xi = 1.0$ was filled with a non-uniform mixing motion, while the zone below was stably stratified as described previously. From this and other observations they concluded that $H/R = 1$ is the largest value for which their solution is fully valid.

An Equivalent Virtual Source

Since any actual source has a finite diameter it is necessary to determine the position of a virtual source before using the plume equations. In as much as the shapes of light fixtures are awkward to handle, the actual source and its plume are treated as if they are circular. A typical middle

section of a factory where the total lighting effect on the floor is equivalent to a single light fixture is shown in Figure 5 with the various parameters used in the analysis. Again, a steady-state problem is considered. Simple expressions involving the outer radius of the section and the mass flow rate from the cooled space into the plume were written as

$$Q_{hl} = \pi R^2 q_{hl} \quad \text{or} \quad R = \left(\frac{Q_{hl}}{\pi q_{hl}} \right)^{1/2} \quad (32)$$

$$\frac{(1 - F_{rl}) Q_{hl}}{3600} = (1 - F_{rl}) Q_{sl} = \dot{m}_{al} c_a (T_b - T_{ac}) \quad (33)$$

The character of a thermal plume source depends only on the buoyancy flux and the volume flux it provides. In terms of the parameters of the light fixture these quantities become

$$\text{Volume flux} = \frac{\dot{m}_{al}}{\rho_a} \quad (34)$$

$$\text{Buoyancy flux} = \frac{\dot{m}_{al}}{\rho_a} g \frac{(T_b - T_{oal})}{T_{aac}} \quad (35)$$

The reference temperature or density for the buoyancy flux was taken to be that of the air conditioned space. With the assumed Gaussian profiles within the plume, integration of these quantities over the plume section was required. The details of the integration are included in Appendix A and the results are

$$\text{Volume Flux} = \pi b_w^2 w \quad (36a)$$

$$\text{Buoyancy Flux} = \frac{\pi}{2} b_w^2 \Delta \quad (36b)$$

Also, integration over the horizontal plume section yields

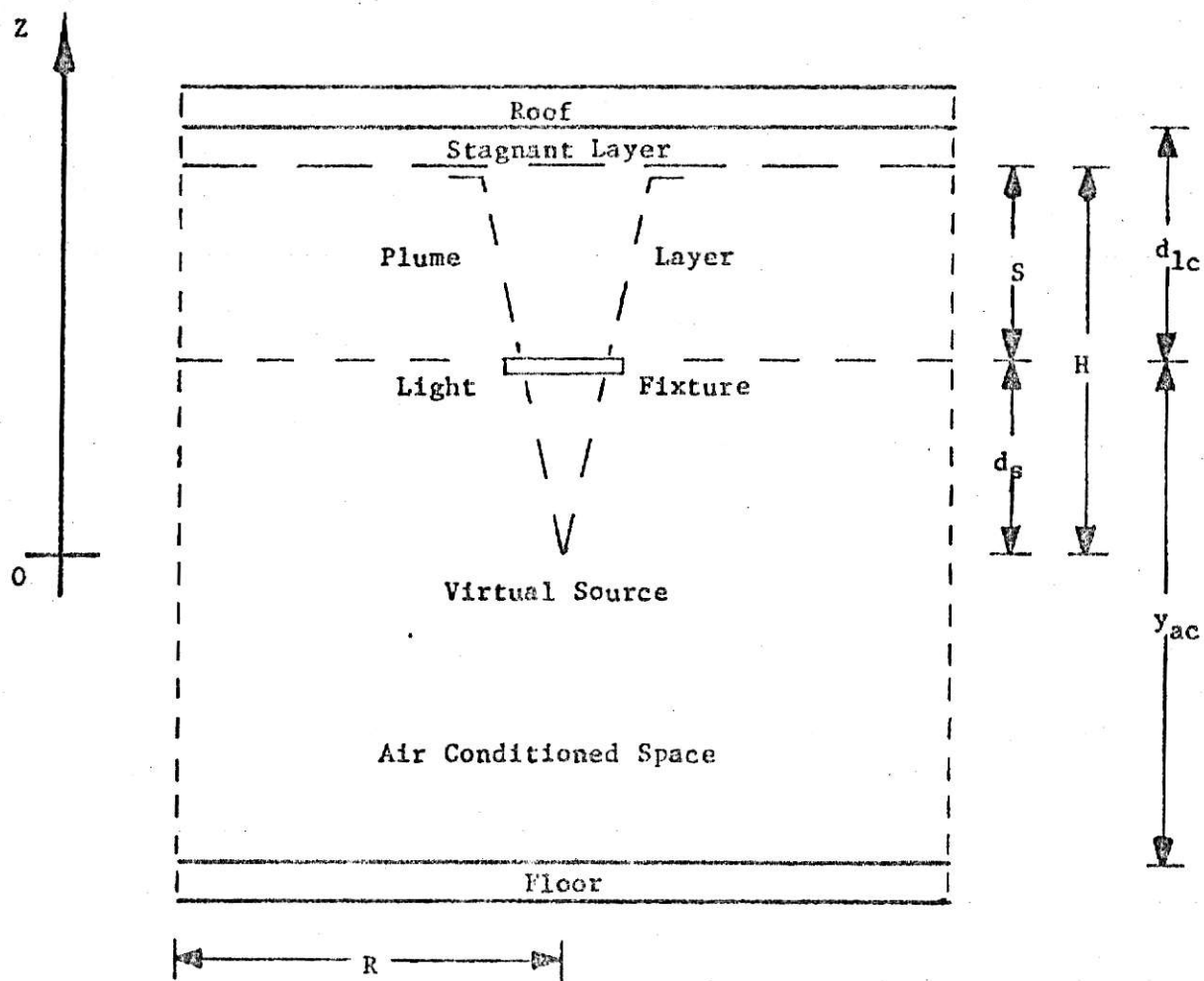


Figure 5. Typical Middle Section of a Factory Where the Lighting Effects Are Equivalent to a Single Light Fixture.

$$d_s = \frac{(0.253 \dot{m}_{al} / \rho_a)^{3/5}}{\alpha^{4/5} F_o^{1/5}} \quad (41)$$

Equation (41) gives an approximate value for d_s in terms of known quantities of the actual source and the entrainment constant.

For the case of the plume in a confined region the buoyancy flux is not constant with height. Therefore, the values of both d_s and F_o must be obtained for an equivalent virtual source. Substituting equations (18) - (20) into (38) and (39) produced

$$\frac{\dot{m}_{al}}{\rho_a} = 4\pi^{2/3} \alpha^{4/3} H^{5/3} F_o^{1/3} (-j) \quad (42)$$

$$F_{as} = \frac{\dot{m}_{al}}{\rho_a} g \frac{(T_b - T_{oal})}{T_{aac}} = F_o \left(\frac{S}{S + d_s} \right) \quad (43)$$

Equation (43) implies that the buoyancy flux decreases linearly as height increases, which is also apparent after a close inspection of (30). After cubing (42) and solving (43) for F_o and combining, it was found that

$$\frac{64 \pi^2 \alpha^4 g}{(\dot{m}_{al} / \rho_a)^2 S} \frac{(T_b - T_{oal})}{T_{aac}} (S + d_s)^6 (-j(\xi_s))^3 - 1 = 0 \quad (44)$$

where $\xi_s = \frac{d_s}{S + d_s}$. Once the value of d_s , which is a root of (44) is known

F_o can be computed from (43).

$$T_b - T_{oal} = 1/2 (T_m - T_{oal}) \quad (37)$$

Equating (34) with (36a) and (35) with (36b) gives

$$\frac{\dot{m}_{al}}{\rho_a} = \pi b^2 w \quad (38)$$

$$\frac{\dot{m}_{al}}{\rho_a} g \frac{(T_b - T_{oal})}{T_{aac}} = \frac{\pi}{2} b^2 w \Delta \quad (39)$$

Neglecting the density changes with height in the environment an approximation of the position of the virtual source was obtained from the solution of the plume equations in a uniform environment, (11) - (14). The use of the series solution, (17) - (21) and (28) - (31), was clumsy and produced a non-linear equation whose roots must be determined by a numerical scheme. An initial estimate of d_s is provided by the approximation for uniform environment and is required by any iterative method. Therefore, both equations are needed and their derivations follow.

The buoyancy flux for a plume in uniform surroundings is constant with height. Comparing (11) with (39) shows that the value of F_o can be computed if the values of the parameters on the right hand side of (39) are known for the actual source. An expression for d_s was found by solving (38) for w and equating it with (13). After substitution of (12) in place of b it was found that

$$w(d_s) = \frac{\dot{m}_{al}}{\pi(6/5)^2 \alpha^2 d_s^2 \rho_a} = \frac{5}{6} \left(\frac{18}{5\pi} \alpha F_o \right)^{1/3} d_s^{-1/3} \quad (40)$$

Solving (40) for d_s and reducing the expression gave

$$d_s = \frac{(0.253 \dot{m}_{al} / \rho_a)^{3/5}}{\alpha^{4/5} F_o^{1/5}} \quad (41)$$

Equation (41) gives an approximate value for d_s in terms of known quantities of the actual source and the entrainment constant.

For the case of the plume in a confined region the buoyancy flux is not constant with height. Therefore, the values of both d_s and F_o must be obtained for an equivalent virtual source. Substituting equations (18) - (20) into (38) and (39) produced

$$\frac{\dot{m}_{al}}{\rho_a} = 4\pi^{2/3} \alpha^{4/3} H^{5/3} F_o^{1/3} (-j) \quad (42)$$

$$F_{as} = \frac{\dot{m}_{al}}{\rho_a} g \frac{(T_b - T_{oal})}{T_{aac}} = F_o \left(\frac{S}{S + d_s} \right) \quad (43)$$

Equation (43) implies that the buoyancy flux decreases linearly as height increase which is also apparent after a close inspection of (30). After cubing (42) and solving (43) for F_o and combining, it was found that

$$\frac{64 \pi^2 \alpha^4 g}{(\dot{m}_{al} / \rho_a)^2 S} \frac{(T_b - T_{oal})}{T_{aac}} (S + d_s)^6 (-j(\xi_s))^3 - 1 = 0 \quad (44)$$

where $\xi_s = \frac{d_s}{S + d_s}$. Once the value of d_s , which is a root of (44) is known

F_o can be computed from (43).

Rejection of Ventilation Air Through the Stratified Layer

Consider the steady-state downward velocity profile of the surrounding air in the plume layer given by (21) and (28). Let a stagnant layer be present between the ceiling and the plume layer. Furthermore, suppose roof ventilation fans which draw air from the air conditioned space through the stratified layer are operating. Assume that the fans were not placed directly over the rising plumes but are located above the surrounding air which is under most of the ceiling area. Then, the entrainment rate at any level of the undisturbed plume is identical with the case of no ventilation and the same environmental temperature profile.

Superposition of the uniform upward velocity of the ventilation air with the original velocity profile given by (21) and (28) in the plume layer yields

$$U_{pl}(\xi) = 3600 (V + U_s(\xi)) \quad (45)$$

Neglecting the relatively small volume of air directly above the rising plume, the velocity throughout the stagnant layer becomes

$$U_{sl} = 3600 V \quad (46)$$

Transient Energy Equations

The plume equations for the velocity profile of the surrounding air in the plume layer, (21), (28) and (45), provide a steady-state solution. However, the problem considered in this study is of transient nature since the roof load changes with time. A transient equation of the surrounding air was desired which, together with the plume equations, could be solved by numerical methods. Also, the transient energy equations for the stagnant layer, the roof and the floor along with appropriate boundary conditions were needed. These equations

give a concise statement of the problem but the boundary conditions of the plume layer are awkward. The numerical treatment easily handles the boundary conditions but is much more lengthy.

The vertical coordinate within the factory was taken to be y , as shown in Figure 6, since the coordinate system used in the discussion of the thermal plumes is not convenient. Comparison of Figures 5 and 6 yields the coordinate transformation,

$$z = y_{ac} - d_s + y \quad (47)$$

For the derivation of the energy equation of the surrounding air of the plume layer, consider a one dimensional spatial element with dimension d_y .

In making an energy balance on this element only the following forms of energy were assumed significant:

1. Internal energy of the fluid.
2. Heat transferred by conduction.
3. Heat transferred by convection.

The various energy rates for making the energy balance are listed in Table 1 and are shown with the spatial element in Figure 7. Making the energy balance and reducing yields

$$\begin{aligned} \rho_a c_a \frac{\partial T_{pl}}{\partial t} &= k_a \frac{\partial^2 T_{pl}}{\partial y^2} - \rho_a c_a \frac{(U_{pl} T_{pl})}{\partial y} - \rho_a c_a v T_{pl} \\ &= k_a \frac{\partial^2 T_{pl}}{\partial y^2} - \rho_a c_a \left[U_{pl} \frac{\partial T_{pl}}{\partial y} + T_{pl} \left(\frac{\partial U_{pl}}{\partial y} + v \right) \right]. \end{aligned} \quad (48)$$

Similarly, a mass balance gives

$$\frac{\partial U_{pl}}{\partial y} + v = 0 \quad (49)$$

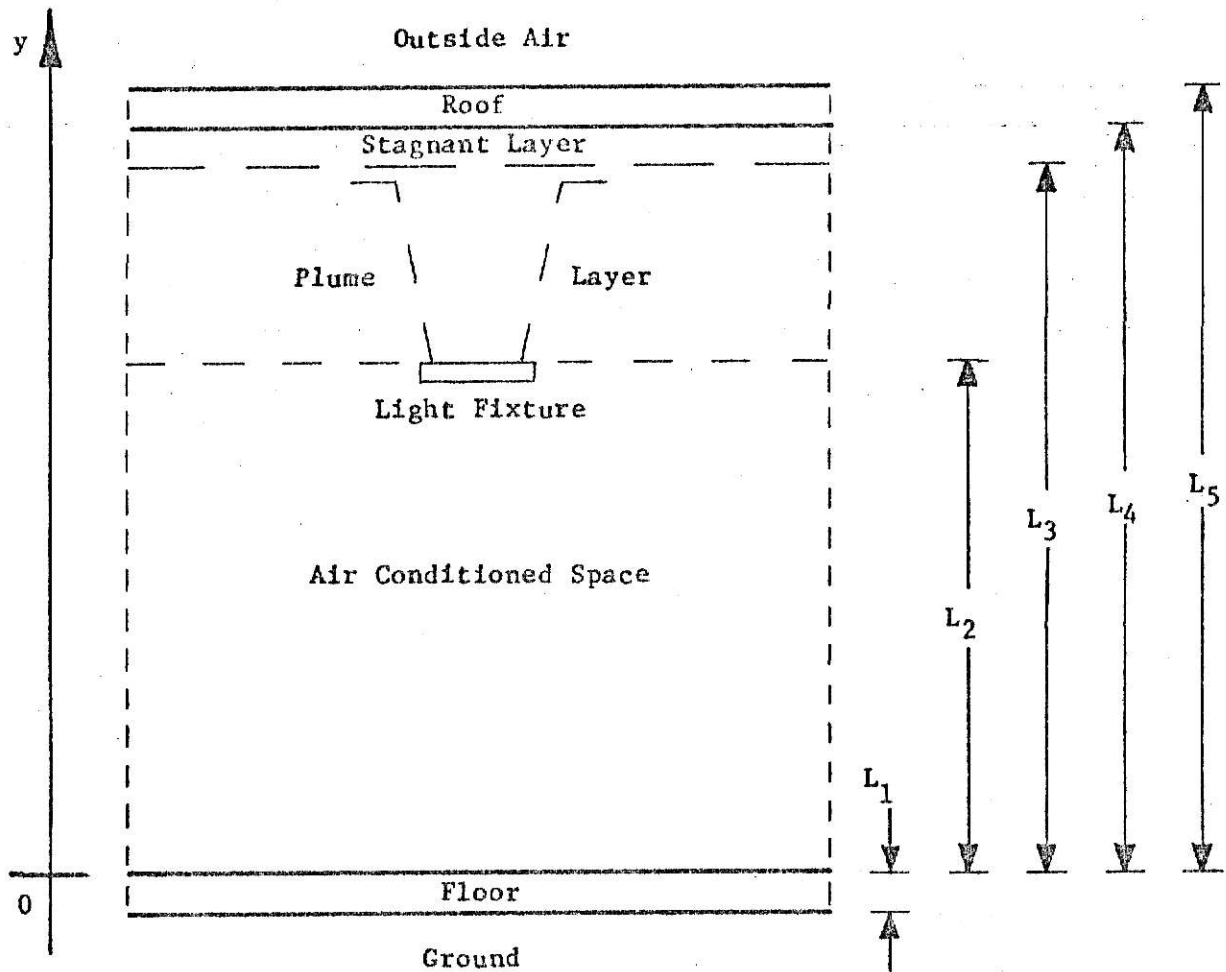


Figure 6. Vertical Coordinate System for the Middle Section of the Factory.

TABLE I

Energy Rates on a Spatial Element of the Surrounding Air of the Plume Layer

| Form of Energy Rate | Symbol | Expression |
|--|--|---|
| Internal Energy Stored | q_{st} | $\rho_a c_a \frac{\partial T_{pl}}{\partial t} dy$ |
| Conduction with surrounding air at y | q_{cd} | $-k_a \frac{\partial T_{pl}}{\partial y}$ |
| Conduction with surrounding air at y + dy | $q_{cd} + \frac{\partial q_{cd}}{\partial y} dy$ | $-k_a \frac{\partial T_{pl}}{\partial y} - k_a \frac{\partial^2 T_{pl}}{\partial y^2} dy$ |
| Convection with surrounding air at y | q_{cv} | $\rho_a c_a U_{pl} T_{pl}$ |
| Convection with surrounding air at y + dy | $q_{cv} + \frac{\partial q_{cv}}{\partial y} dy$ | $\rho_a c_a U_{pl} T_{pl} + \rho_a c_a \frac{\partial (U_{pl} T_{pl})}{\partial y} dy$ |
| Convection from plume entrainment | q_{cvp} | $\rho_{vc} c_a T_{pl} dy$ |

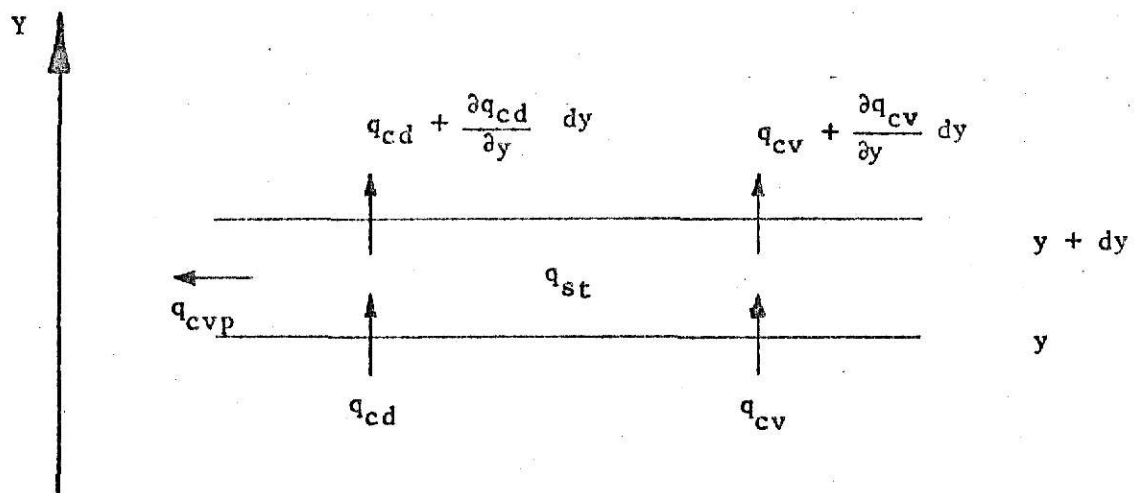


Figure 7. A Spatial Element of the Surrounding Air in the Plume Layer.

Substitution of (49) into (48) produces the desired equation as

$$U_{pl} \frac{\partial T_{pl}}{\partial y} + \frac{\partial T_{pl}}{\partial t} = \alpha_a \frac{\partial^2 T_{pl}}{\partial y^2} , \quad L_2 < y < L_3 \quad . \quad (50)$$

Equation (50) contains a non-linear term, $U_{pl} \frac{\partial T_{pl}}{\partial y}$, since $U_{pl} = U_{pl}(y, T_{pl})$, i.e., the velocity in the surrounding air determined by the plume equations depends on the temperature distribution within the stratified layer.

Conduction heat transfer between the plume layer and the air conditioned space cannot readily be expressed as a boundary condition at $y = L_2$ because the imaginary boundary in the physical model has no thickness. The boundary condition at $y = L_3$ includes the injection of the plume air at its bulk temperature at that level and conduction between the stagnant layer and plume layer. In the case when no stagnant layer is present convection between the ceiling and the plume layer is the proper boundary condition. These conditions were not expressed in equation form here since some are awkward, but they are an essential part of the numerical solution.

The energy equation and boundary conditions for the stagnant layer were written as

$$U_{sl} \frac{\partial T_{sl}}{\partial y} + \frac{\partial T_{sl}}{\partial t} = \alpha_a \frac{\partial^2 T_{sl}}{\partial y^2} , \quad L_3 < y < L_4 \quad (51)$$

$$k_a \frac{\partial T_{sl}}{\partial y} = k_a \frac{\partial T_{pl}}{\partial y} , \quad y = L_3 \quad (52)$$

$$k_a \frac{\partial T_{sl}}{\partial y} = h_c (T_r - T_{sl}) , \quad y = L_4 \quad . \quad (53)$$

The ceiling and the floor were considered as two infinite parallel planes where the radiation shape factor is unity since all the radiation heat transfer leaving one plane reaches the other. The radiation heat flow rate per unit area was written as

$$q_{\text{rad}} = \frac{\sigma (T_r^4(L_4, t) - T_f^4(L_1, t))}{1/\epsilon_c + 1/\epsilon_f - 1}$$

A radiation coefficient was defined for convenience to express the radiation heat transfer in terms of the linear temperature difference $T_r(L_4, t) - T_f(L_1, t)$. Thus,

$$q_{\text{rad}} = h_r (T_r(L_4, t) - T_f(L_1, t)) \quad (54)$$

where

$$h_r = \frac{\sigma (T_r^4(L_4, t) - T_f^4(L_1, t))}{(1/\epsilon_c + 1/\epsilon_f - 1) (T_r(L_4, t) - T_f(L_1, t))} \quad (55)$$

The boundary condition at the outside of the roof varies with time in a 24 hour cycle and can be expressed by the sol-air temperatures described in the ASHRAE Handbook of Fundamentals (12). Below the floor the ground receives heat by conduction and it was treated as an infinite heat sink since its temperature remains unchanged below a certain depth. For simplicity here, consider a floor and roof which are each composed of a homogenous material although multilayer construction was easily handled in the numerical solution. The one dimensional transient heat conduction equation and boundary conditions for the roof and floor were written as

$$\frac{\partial T_r}{\partial t} = \alpha_r \frac{\partial^2 T_r}{\partial y^2}, \quad L_4 < y < L_5 \quad (56)$$

$$k_r \frac{\partial T_r}{\partial y} = h_c (T_r - T_{sl}) \quad , \quad y = L_4 \quad (57)$$

$$k_r \frac{\partial T_r}{\partial y} = h_s (T_{sat}(t) - T_r) \quad , \quad y = L_5 \quad (58)$$

$$\frac{\partial T_f}{\partial t} = \alpha_f \frac{\partial^2 T_f}{\partial y^2} \quad , \quad -L_1 < y < 0 \quad (59)$$

$$k_f \frac{\partial T_f}{\partial y} = C_g (T_f - T_g) \quad , \quad y = -L_1 \quad (60)$$

$$k_f \frac{\partial T_f}{\partial y} = h_f (T_f - T_{ac}) + h_r (T_r(L_4, t) - T_f(L_1, t)) + F_{rl} q_{hl} \quad , \quad y = 0 \quad (61)$$

The Heat Flow Rates

Consider a known temperature profile of the factory at time t . The equations for a horizontal unit area were written describing the heat flow rates given in Figure 8 where the arrows indicate positive direction. From the boundary conditions listed in the previous section,

$$q_{roof} = h_s (T_{sat}(t) - T_r(L_5, t)) \quad (62)$$

$$q_{ce11} = h_c (T_r(L_4, t) - T_{sl}(L_4, t)) \quad (63)$$

$$q_{rad} = h_r (T_r(L_4, t) - T_f(L_1, t)) \quad (54)$$

$$q_{flin} = h_f (T_f(L_1, t) - T_{ac}) \quad (64)$$

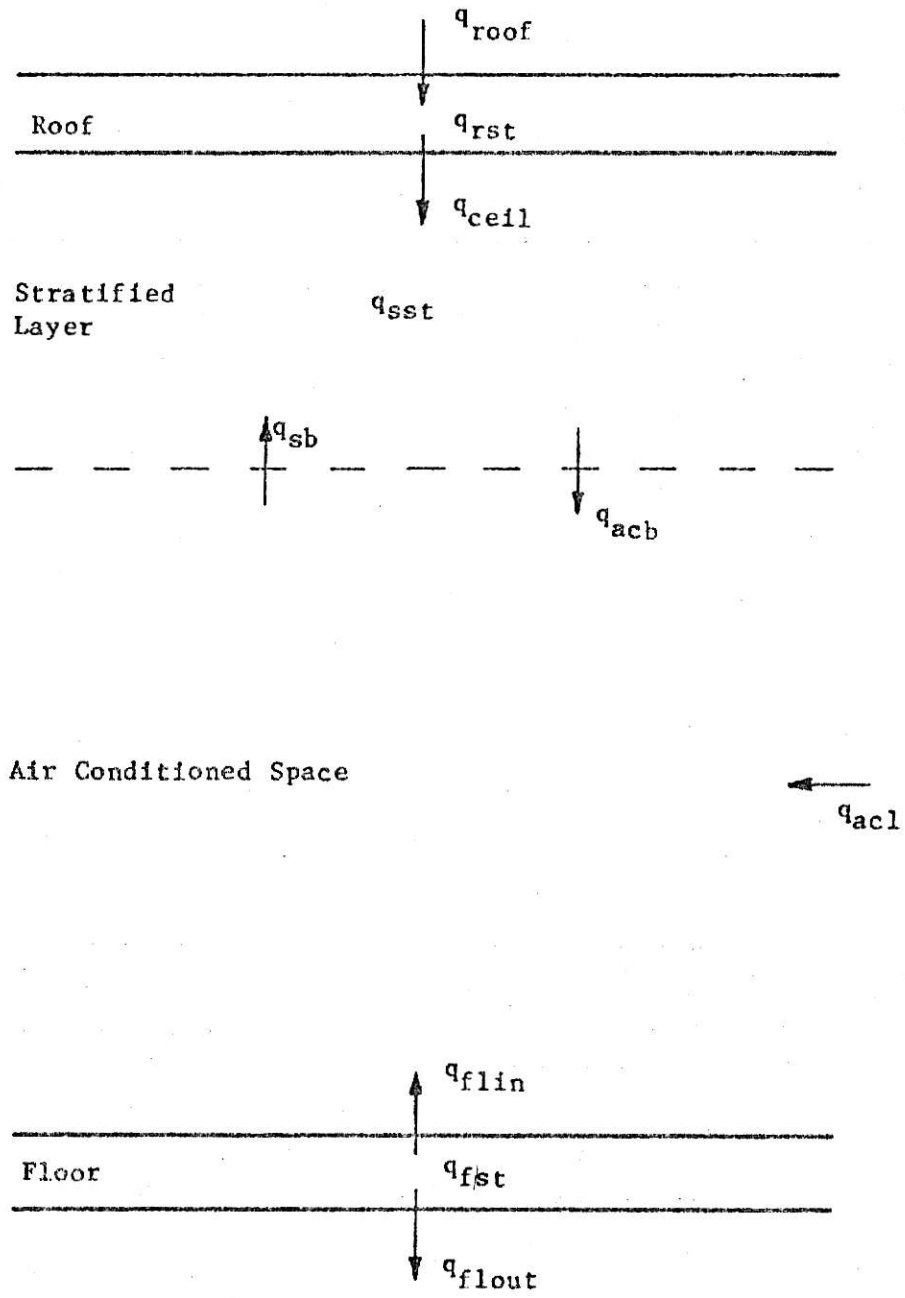


Figure 8. Direction of Heat Flows.

$$q_{flout} = C_g (T_f(0, t) - T_g) \quad (65)$$

Energy balances on the floor and the roof gave

$$q_{rst} = q_{roof} - q_{ceil} - q_{rad} \quad (66)$$

$$q_{flst} = q_{rad} - q_{flin} - q_{flout} + F_{rl} q_{hl} \quad (67)$$

The heat flow rates due to the fluid motion of the plume and the ventilation air remain to be listed. The total ventilation heat load on the air conditioning system is the sum of the sensible heat gain corresponding to the change of dry-bulb temperature for the given air flow and the latent heat gain corresponding to a change of humidity ratio. The two cases with or without exhausting ventilation air through the stratified layer were considered separately. For the case without rejection of ventilation air through the stratified layer the heat flow rates were written as

$$q_{sb} = - \rho_a U_h(\xi_s) c_a (T_b - T_{pl}(L_2, t)) \quad (68a)$$

$$q_{acb} = - \rho_a U_h(\xi_s) c_a (T_{pl}(L_2, t) - T_{ac}) + 60 \rho_a Q_v c_a (T_{oa}(t) - T_{ac}) + 4840 Q_v \Delta W \quad (69a)$$

The last two terms in (69a) correspond to the sensible and latent heat gain for the ventilation air flow as described in the ASHRAE Handbook of Fundamentals (12). In both (68a) and (69a), $- \rho_a U_h(\xi_s)$ represents the mass of air per unit area from the air conditioned space feed into the plume. When ventilation air is exhausted through the stratified layer two cases, $U_{pl}(\xi_s)$ negative (downward) and $U_{pl}(\xi_s)$ positive (upward), were treated separately. For negative

$U_{pl}(\xi_s)$ the heat flow rates were written as

$$q_{sb} = \rho_a c_a \left[-U_h(\xi_s) T_b + U_{pl}(\xi_s) T_{pl}(L_2, t) - U_{sl} T_{sl}(L_4, t) \right] \quad (68b)$$

$$q_{acb} = -\rho_a c_a \left[-U_h(\xi_s) T_{ac} + U_{pl}(\xi_s) T_{pl}(L_2, t) \right] + 60 \rho_a Q_v c_a (T_{oa}(t) - T_{ac}) + 4840 Q_v \Delta W \quad (69b)$$

The heat flow rates for the case of positive $U_{pl}(\xi)$ were written as

$$q_{sb} = \rho_a c_a \left[-U_h(\xi_s) T_b + U_{pl}(\xi_s) T_{ac} - U_{sl} T_{sl}(L_4, t) \right] \quad (68c)$$

$$q_{acb} = -\rho_a c_a \left[-U_h(\xi_s) T_{ac} + U_{pl}(\xi_s) T_{ac} \right] + 60 \rho_a Q_v c_a (T_{oa}(t) - T_{ac}) + 4840 Q_v \Delta W \quad (69c)$$

Note that the entire convective portion of the heat generated by the lights was assumed to be fed into the plume. Thus, q_{sb} is a measurement of how much of the convective portion of the lighting load remains in the stratified layer. Conduction heat transfer between the plume layer and the air conditioned space was neglected in these heat flow rates but it was included in the numerical solution.

Finally, the heat balances on the stratified layer and the air conditioned space were written as

$$q_{sst} = q_{ceil} + q_{sb} \quad (70)$$

$$q_{acl} = q_{acb} + q_{flin} \quad (71)$$

The quantity q_{ac1} must be provided by the air conditioning system to the cooled space in order to maintain the desired temperature and humidity.

CHAPTER V

NUMERICAL SOLUTION

A numerical solution to the equations developed in the previous section which includes the various modes of heat transfer and the periodic boundary condition at the roof was desired. Newton's method for solving a non-linear equation was used to find the position of the virtual source. Implicit finite difference equations were written which reduced the problem to a set of linear algebraic equations at each time step. The non-linear term in the energy equation of the stratified layer was linearized by treating the velocity profile constant over the time increment. Gauss-Jordan elimination was employed to solve this system of equations. The thickness of the stagnant layer was obtained by a comparison of the incoming bulk plume temperature and surrounding air temperature at each level in the stratified layer. A computer program was written based on these numerical techniques.

Position of the Virtual Source

The parameter d_g of the equivalent virtual source was desired for a given actual source and surrounding temperature at the previous time increment. An initial estimate of d_g is given by equation (41) which was derived from the expressions representing uniform surroundings. The root of equation (44) near the estimated value is needed for an accurate value of d_g .

Equation (44) is in the general form of a non-linear equation written as

$$f(d_g) = 0 \quad . \quad (72)$$

Newton's method is applied with an iteration procedure given by

$$d_s^{u+1} = d_s^u - \frac{f(d_s^u)}{f'(d_s^u)} \quad (73a)$$

where the superscripts enumerate the successive approximations. Evaluation of $f'(d_s^u)$ and $f(d_s^u)$ is required at each $u + 1$ iteration step. Differentiation of equation (44) yields

$$f'(d_s) = \frac{64 \pi^2 \alpha^4 g}{(\dot{m}_{al}/\rho_a)^2 S} \frac{(T_b - T_{oal})}{T_{aac}} \left[6 (S + d_s)^5 (-j(\xi_s))^3 + 3 (S + d_s)^6 (-j(\xi_s))^2 \frac{d}{d d_s} (-j(\xi_s)) \right] \quad (73b)$$

$$\text{where } \frac{d}{d d_s} (-j(\xi_s)) = \frac{S}{(S + d_s)^2} \left(0.765 \xi_s^{2/3} - 0.157 \xi_s^{5/3} - 0.0367 \xi_s^{8/3} \right) .$$

Issacson and Keller (13) discussed the conditions for convergence of Newton's method while proving several applicable theorems. Let

$$d_s = g(d_s) = d_s - \frac{f(d_s)}{f'(d_s)} .$$

Note that $g(d_s)$ has roots which coincide with those of (72) and no others. A sufficient condition for convergence on any closed interval containing a root at $d_s = \gamma$ is that $g(d_s)$ satisfies the Lipschitz condition on the closed interval,

$$| g(d_s) - g(\gamma) | \leq \lambda | d_s - \gamma |$$

where $\lambda < 1$. This condition is satisfied and the procedure will converge if the initial estimate is sufficiently close to a root.

In actual computations roundoff errors in the evaluation of the functions limit the size of the error band independently of the number of iterations. Any test for the termination of the iterations should allow for this roundoff effect. Since only three significant digit accuracy was desired no complications were encountered with the simple convergence test

$$| d_s^v - d_s^{v+1} | < 0.01 \quad .$$

Finite Difference Procedure

The energy equations for the surrounding air in the stratified layer, the roof and the floor given by (50), (51), (56) and (56) were solved by finite difference methods. The implicit method was used since it is stable regardless of the size of the time increment used. The vertical space of the factory was divided into nodes and difference equations were derived by applying a heat balance to each node of horizontal, unit area. The non-linear term, $U_{pl} \frac{\partial T_{pl}}{\partial y}$, in (50) was linearized by considering the velocity components to be known and they were taken equal to their values at the previous time level. That is, the values of T_{oal} and S were used in the plume equations from the temperature profile at the previous time level. Conduction heat transfer between the stratified layer and the air conditioned space and the thermal storage of the structural steel near the ceiling were included in the difference equations. Modification of the nodal equations for each value of S is necessary.

In the daily cycle of some factories a shut down period may occur during a portion of the day in the early morning. Since the air conditioning

system, factory equipment and lights are off during this period, the desired temperature of the air conditioned space is no longer maintained. An extra difference equation was added to the previous set to be solved for the changing temperature of the lower space. A listing of the difference equations is provided in Appendix B.

The implicit nodal equations form a set of linear algebraic equations which must be solved simultaneously. In the usual matrix notation the problem is

$$Ax = f$$

where A is a square matrix and x and f are column vectors. For the present problem, A resembles a tridiagonal matrix with a partial row and two other coefficients symmetrically added. The partial row changes position when the value of S changes. Since the majority of coefficients are zero, the computer program employing Gauss-Jordan elimination was written to skip them. A relatively small number of equations, usually about 15, were solved.

Error Analysis

The numerical procedure outlined above contains two distinct kinds of error. First, the discretization error is due to the basic approximation of replacing the differential equation by algebraic equations of discrete quantities. Second, the roundoff error is a computational error caused by only a finite number of decimals being retained after rounding. Both of these errors require some further explanation.

An equivalent method for derivation of difference equations is replacing space and time derivatives with finite differences obtained by algebraic elimination of truncated Taylor series expansions about several adjacent points. The order of the discretization error with respect to a space or time increment is obtained by this approximation. Such a procedure is

explained by the authors of most texts on numerical analysis including Crandall (15). Similarly, a Taylor series expansion was applied to find the order of error introduced by the linearization of a term in a non-linear partial differential equation by Barakat and Clark (8). Consider the term $U_{pl} \frac{\partial T_{pl}}{\partial y}$ in (50). If U_{pl}^t and U_{pl}^{t+1} are the values of the velocity at time levels t and $t+1$ respectively, then

$$U_{pl}^{t+1} \frac{\partial T_{pl}}{\partial y} = U_{pl}^t \frac{\partial T_{pl}}{\partial y} + \Delta t \left(\frac{\partial U_{pl}}{\partial t} \right) \frac{\partial T_{pl}}{\partial y} . \quad (74)$$

The last term on the right side of equation (74) represents the linearization error which is of order $O(\Delta t)$. Thus, the discretization and linearization errors can be reduced by decreasing the size of space or time increments.

Next consider the determination of the magnitude of the roundoff error due to the Gauss-Jordan elimination process. An energy balance for the overall system is a meaningful test of a calculated solution. Little extra work is needed since the quantities required in the energy balance are part of the solution being sought. Clausing (14) discussed the uses of such an energy balance which include a criterion for the termination of an iterative method when one is employed, the approximation of the roundoff errors for a direct procedure, and a check on the computer program and the derived set of difference equations. The appropriate overall energy balance in terms of the quantities defined by (54) and (62) - (71) is

$$q_{\text{check}} = q_{\text{roof}} - q_{\text{flout}} + q_{\text{hl}} - q_{\text{acl}} - q_{\text{rst}} - q_{\text{fst}} - q_{\text{sst}} = 0 \quad (75)$$

Thickness of the Stagnant Layer

Determination of the position of the boundary between the stagnant layer and plume layer was carried out at each time step. At the light fixture level T_m was given and T_b was computed by equation (37) with the value of T_{oal} at the current time step ($T_{oal} = T_{pl}(L_2, t)$). The bulk plume temperature at each node level was calculated by a simple heat balance of the rising plume mass from the previous node and the mass of entrainment within the node. Thus, the bulk plume temperature at each node was calculated in the plume layer of thickness determined from the previous time step. If the plume extends into a node, the bulk temperature of the rising plume air from the previous node must be greater than the surrounding at that nodal level. Starting at the light level and proceeding upward with this comparison yielded the thickness of the plume layer at the current time step. Then, it was used at the next time step to compute the nodal temperatures of the surrounding air in the stratified layer.

Procedure of the Computer Program

A brief description of the computer program is presented below containing the order of succession of the calculations. A complete listing of the Fortran computer program is contained in Appendix C. The following sequence of steps was used at each time increment:

1. The buoyancy and volume flux at the light level were evaluated by equations (33) - (34) using the value of T_{oal} at the previous time step.
2. The values of d_s and F_o for the equivalent virtual source were determined from equations (41), (43), (44) and (73).

3. The velocity profile in the plume layer was computed using (21) and (28). If ventilation air was exhausted through the stratified layer it was superimposed on the plume fluid motion by (45) and (46).
4. The coefficients in the difference equations were calculated and arranged in a two dimensional array.
5. These equations were solved by Gauss-Jordon elimination for the nodal temperatures.
6. The bulk plume temperatures were determined and the comparisons were performed to establish the boundary between the plume and stagnant layers.
7. The heat flow rates including q_{acl} were evaluated using equations (54) and (62) - (71).

CHAPTER VI

RESULTS AND DISCUSSION

The daily cycle of the factory was simulated by the computer program employing the numerical techniques of the previous chapter. Since the initial temperature profile was unknown, a constant temperature distribution of T_{ac} was assumed. Within a 48 hour period containing two daily cycles excellent agreement developed between the end of the first cycle and the end of the second. Thus, a 48 hour run was sufficient to produce an appropriate initial condition.

The overall energy balance, (75), revealed that the roundoff error in the Gauss-Jordan elimination was small because the maximum absolute value encountered of q_{check} was only 0.001. An approximation to the magnitude of the discretization errors was obtained by varying the space and time increments for some trial computer runs. Upon reducing the time increment from 1 hour to 0.5 hour the maximum difference of temperature over the generated profiles was 0.4 F. Since any decrease in the final space increments produced even less variations, the calculations acquired with hourly spacing were probably in error by less than one degree Fahrenheit. The roundoff error was small compared to this.

The results given by the computer program were compared to data taken from a plant using a thermal stratification system. Further solutions were obtained by varying parameters in the model. These include the effects of exhausting ventilation air through the stratified layer and increasing d_{lc} .

Comparison With the Plant Data

Data from an actual plant with an air conditioning system designed for thermal stratification in Kansas City, Missouri was provided by Dean (2). The air conditioning load of the factory was approximated from observations of the unloader configurations of the air conditioning system. Also, temperature profiles at various times during the daily cycle were measured on an August day. At the beginning of the daily cycle the air conditioning system, along with the rest of the factory equipment, was turned off from midnight to 7 am.

For a meaningful comparison the heat gain through the walls and the internal load due to the people and equipment around the floor were included in the air conditioning load. Thus,

$$\bar{q}_{\text{tot}} = \frac{A_f}{12,000} q_{\text{acl}} + \bar{q}_{\text{wall}} + \bar{q}_{\text{int}} \quad (76)$$

In this factory the ventilation air is supplied and exhausted through the air conditioning system and does not influence the stratified layer above the air conditioning space. Since only design conditions for the computation of the latent gain of the ventilation air were available, the latent gain was assumed constant and equal to the design conditions. However, outdoor air temperatures were used to calculate the changing sensible gain at each time step. A listing of the values used in the comparison is provided in Appendix D.

The only parameter needed for the comparison which remained unknown was the maximum temperature in the plume at the actual source, T_m . Noting that the light fixtures have a bulb surface temperature of approximately 105°F according to Dean, values of 100°F and 90°F were tried. The calculated results along with the measured factory data of the total air conditioning

load are shown in Figure 9. Very little difference in the computed load resulted from the two different values of T_m . However, the measured load was greater than the computed load throughout the daily cycle with a discrepancy of about 10% at its peak. Among the possible explanations for this difference are the measurements of load were crude and only accurate to the nearest 10 tons at best, the disagreement between values corresponding to the installed equipment and the design values is significant, or there were differences between the actual outside weather conditions and the design conditions. Thus, if all the exact values were known the discrepancy between the two curves may possibly be reduced.

Although no significant difference in the air conditioning load appeared for the two different values of T_m , a large difference was determined in the thickness of the stagnant layer developed, as shown in Figure 10. For $T_m = 90^\circ\text{F}$ the volume flux in the plume at the light level was greater since the corresponding T_b was much lower as can be seen by examining equations (33), (34) and (37). Thus, the downward velocity in the stratified layer at the light level, $U_h(\xi_s)$, was greater. This was offset by a decrease in the temperature of the lower stratified layer due to the thicker stagnant layer. For all further calculations the value $T_m = 100^\circ\text{F}$ was used since the maximum plume temperature is probably close to the bulb surface temperature.

The calculated temperature profiles of the stratified layer are compared to the measured temperatures in Figure 11a, b, c and d. Since the light fixtures are 2 feet below the ceiling the temperature of the air conditioned space is assumed below this level. The maximum disagreement occurred at time = 16 at the ceiling with a temperature difference of about 6°F , although the ceiling temperatures were approximately equal at time = 12.

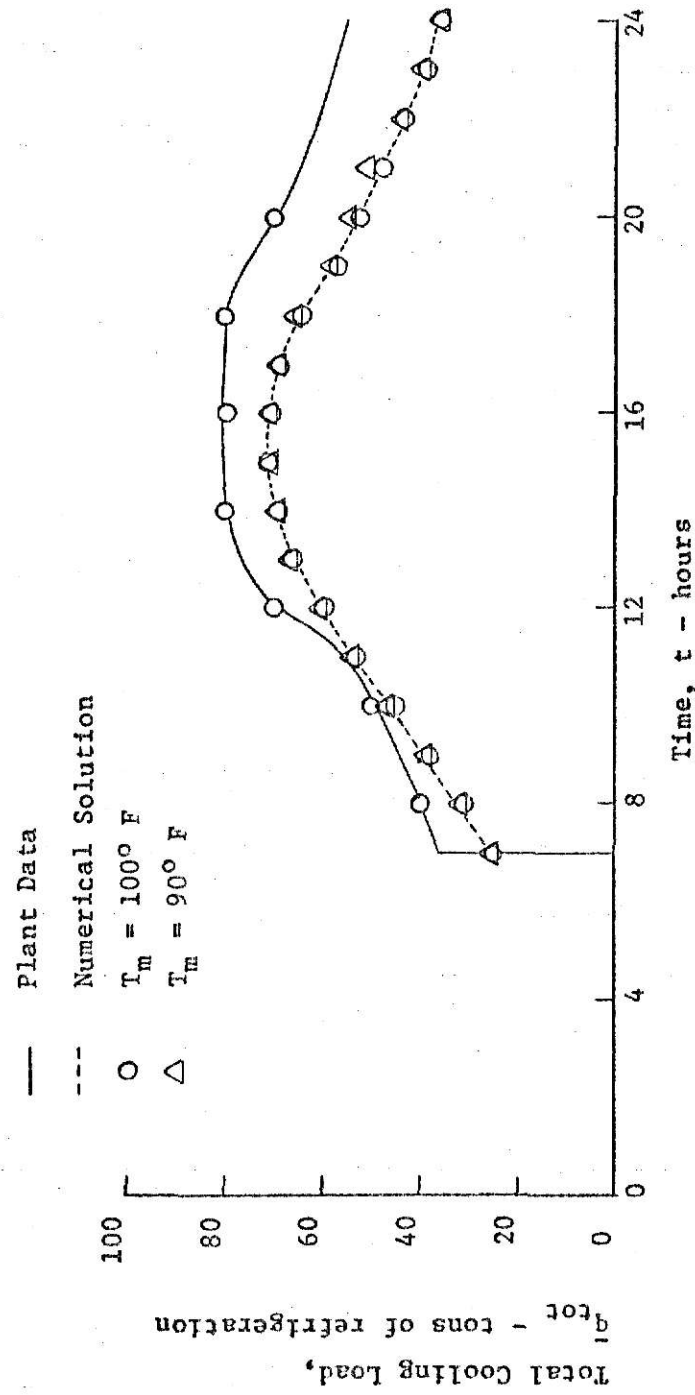


Figure 9. Comparison of Numerical Results with Plant Data for the Total Cooling Load.

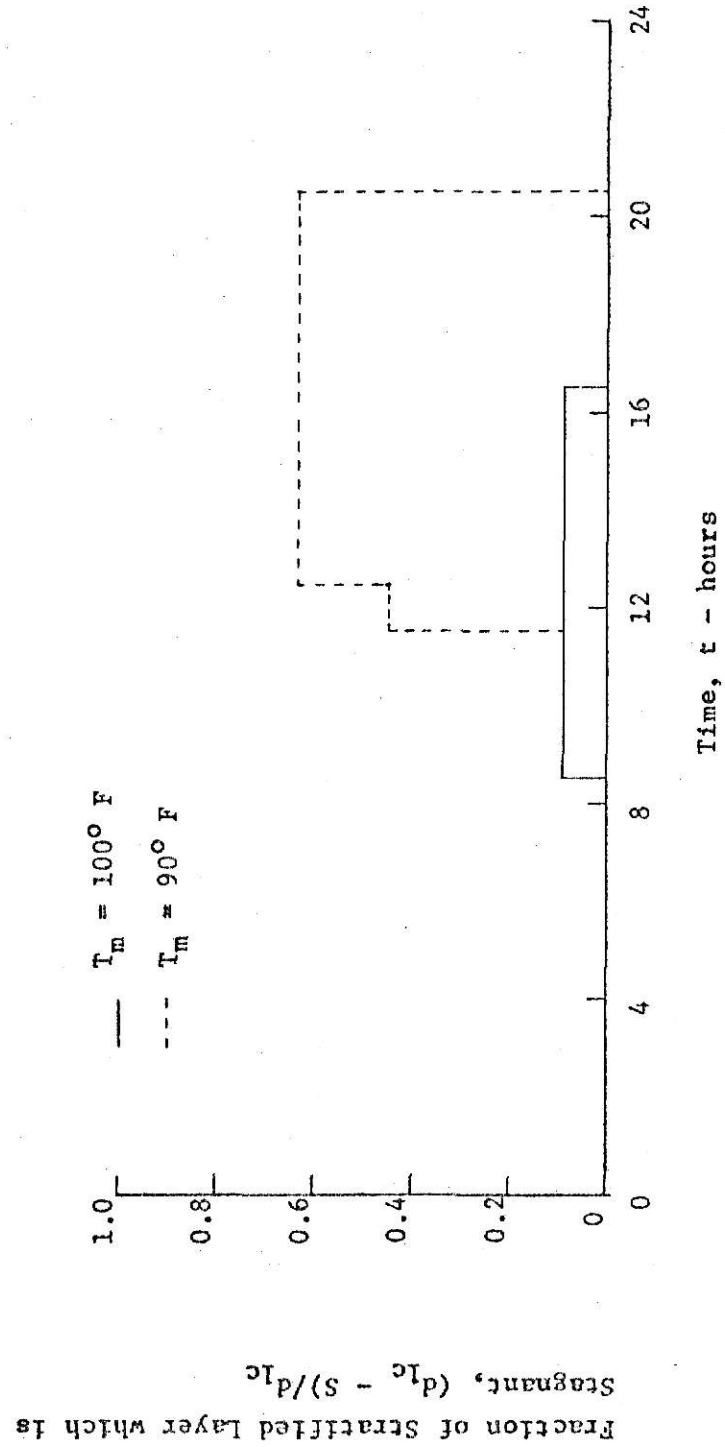


Figure 10. Thickness of the Stagnant Layer For Different Values of T_m

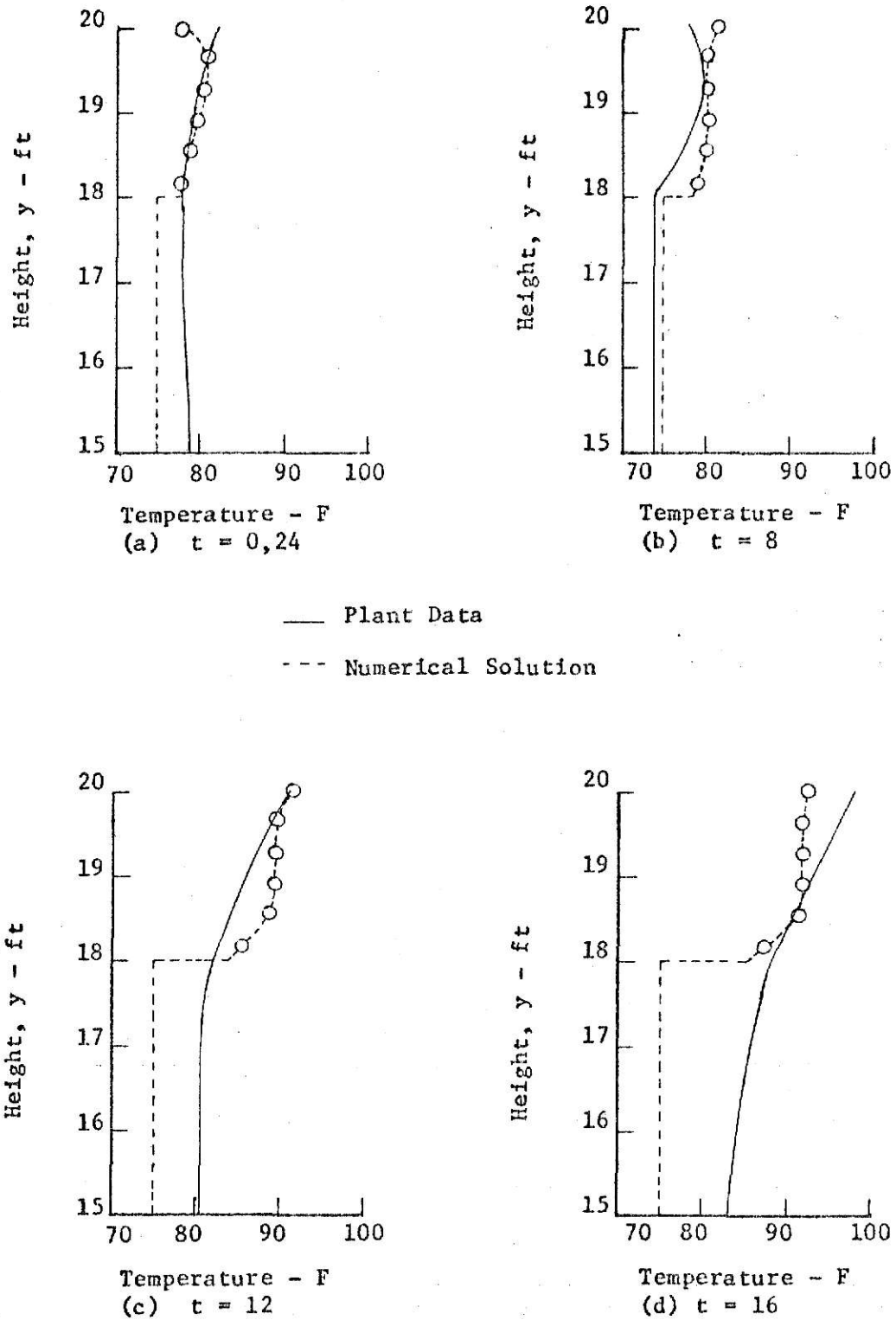


Figure 11. Comparison of Numerical Results with Plant Data for the Temperature Profiles.

Of course, the temperature of the air just below the light level is not equal to T_{ac} in the real case. However, the temperatures in the stratified layer compare reasonably well.

The instantaneous heat flow rates of the various mechanisms of heat transfer and the cumulative thermal storage of the roof, stratified layer and floor over the daily cycle are presented in Figures 12 through 14. It is clear from Figure 12 that the heat transfer between the roof and the outer surroundings was large while convection heat transfer between the ceiling and the stratified layer was practically eliminated. However, the radiant portion of the roof load was significant and part of it entered the air conditioning space through q_{flin} . When the lights were operating q_{sb} was always positive indicating that part of the light load was remaining in the stratified layer. Yet, at the time of peak air conditioning load, time = 14, q_{cb} was approximately zero revealing that nearly all of the convective lighting load, 3 Btu/hr - ft², entered the air conditioned space. Figure 13 shows that conduction heat transfer between the bottom of the floor and the ground was almost constant throughout the daily cycle. Recall

$$q_{acl} = q_{acb} + q_{flin} \quad . \quad (71)$$

The larger contributor to q_{acl} was q_{acb} and most of q_{acb} was due to the sensible and latent heat gains of the ventilation. The cumulative thermal storage of the roof, stratified layer and floor are presented in Figure 14 relative to the energy stored at time = 24. Note that q_{rst} , q_{flst} and q_{sst} are the hourly instantaneous storage rates and the cumulative thermal storages were computed as

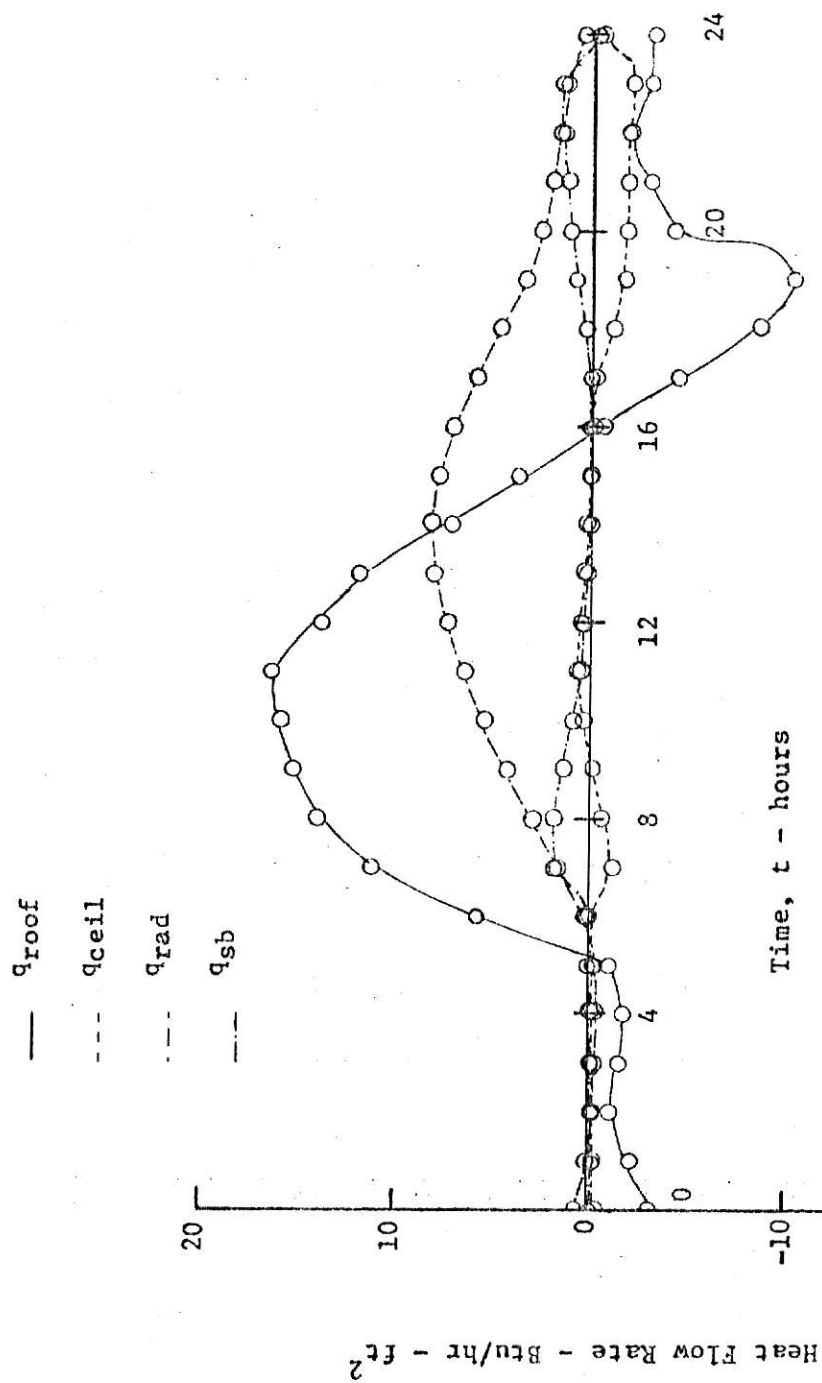


Figure 12. Instantaneous Heat Flow Rates for the Roof and Stratified Layer.

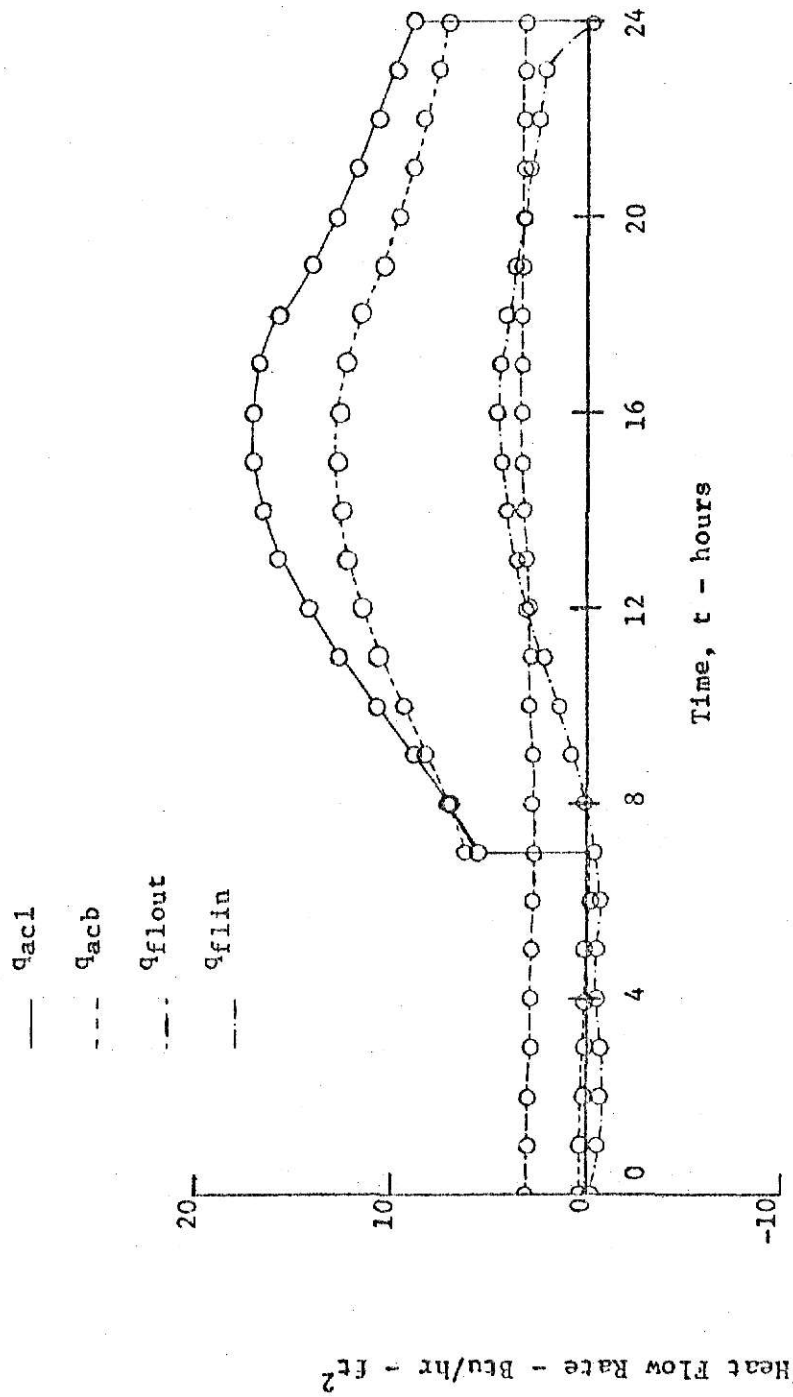


Figure 13. Instantaneous Heat Flow Rates for the Cooled Space and the Floor.

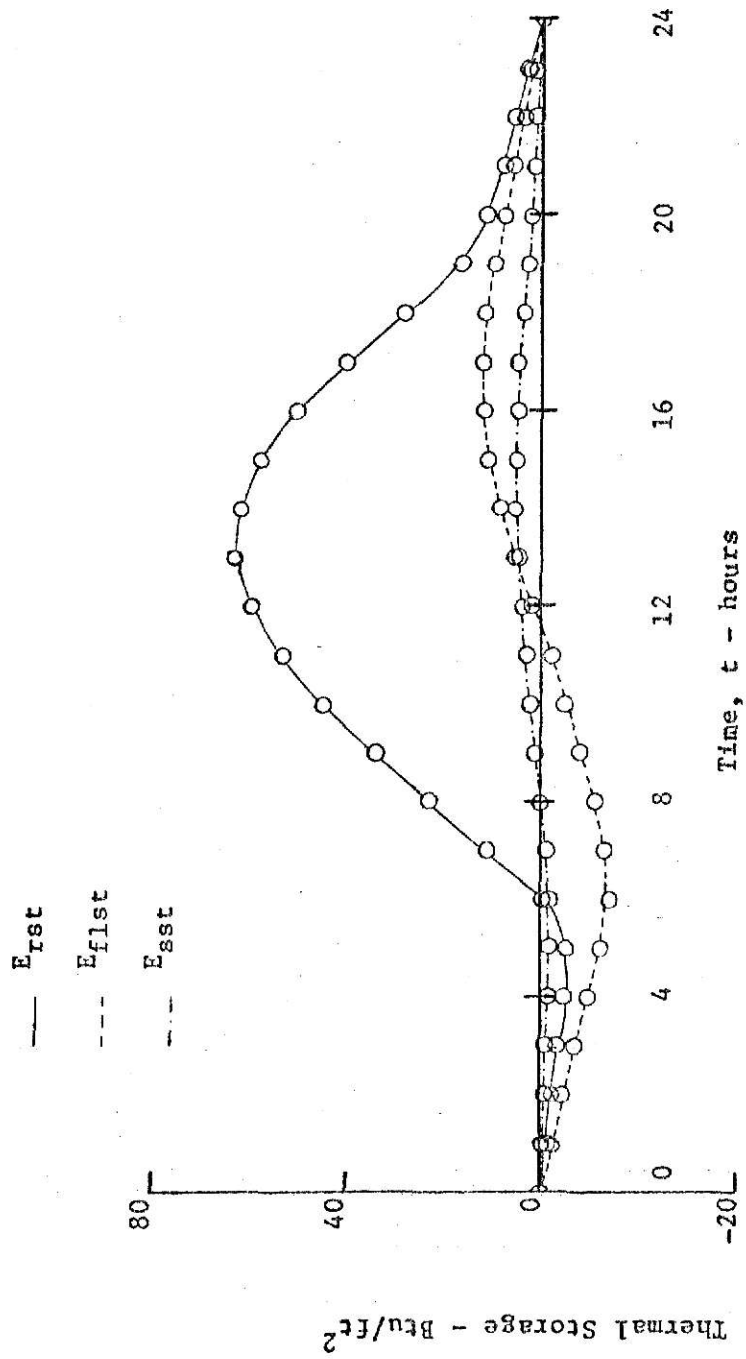


Figure 14. Cumulative Thermal Storage of the Roof, Floor and Stratified Layer.

$$E_{rst}(t) = \sum_{i=1}^t q_{rst}(t) \quad (77a)$$

$$E_{flst}(t) = \sum_{i=1}^t q_{flst}(t) \quad (77b)$$

$$E_{sst}(t) = \sum_{i=1}^t q_{sst}(t) \quad , t = 1, 2, \dots, 24. \quad (77c)$$

The thermal storage of the structural steel was included in E_{sst} but it was small compared to E_{rst} .

Varying Parameters in the Model

Throughout this section the values used in the comparison remained as constants in the model except for the parameters that were changed to obtain a desired comparison. The required air conditioning load was represented by q_{acl} since the effects of thermal stratification in the typical middle section of a factory were studied. In most cases the designer of air conditioning systems is only interested in the peak cooling load, q_{acl}^p , which naturally becomes the important variable. Here the superscript p is used to denote the value of a variable at the time of peak cooling load.

With the same number of light fixtures the results of varying the value of q_{hl} are presented in Figure 15. The results show that any increase in q_{hl} produced nearly the same increase in q_{acl}^p . An additional convective lighting load caused greater mass flows in the plume layer, higher temperatures throughout the stratified layer and a decrease in the thickness of the stagnant layer. Similar to its behavior in the comparison run, the stratified layer retained some of the additional convective lighting load except at the time of peak load.

**THIS BOOK
CONTAINS
NUMEROUS PAGES
WITH MULTIPLE
PENCIL AND/OR
PEN MARKS
THROUGHOUT THE
TEXT.**

**THIS IS THE BEST
IMAGE AVAILABLE.**

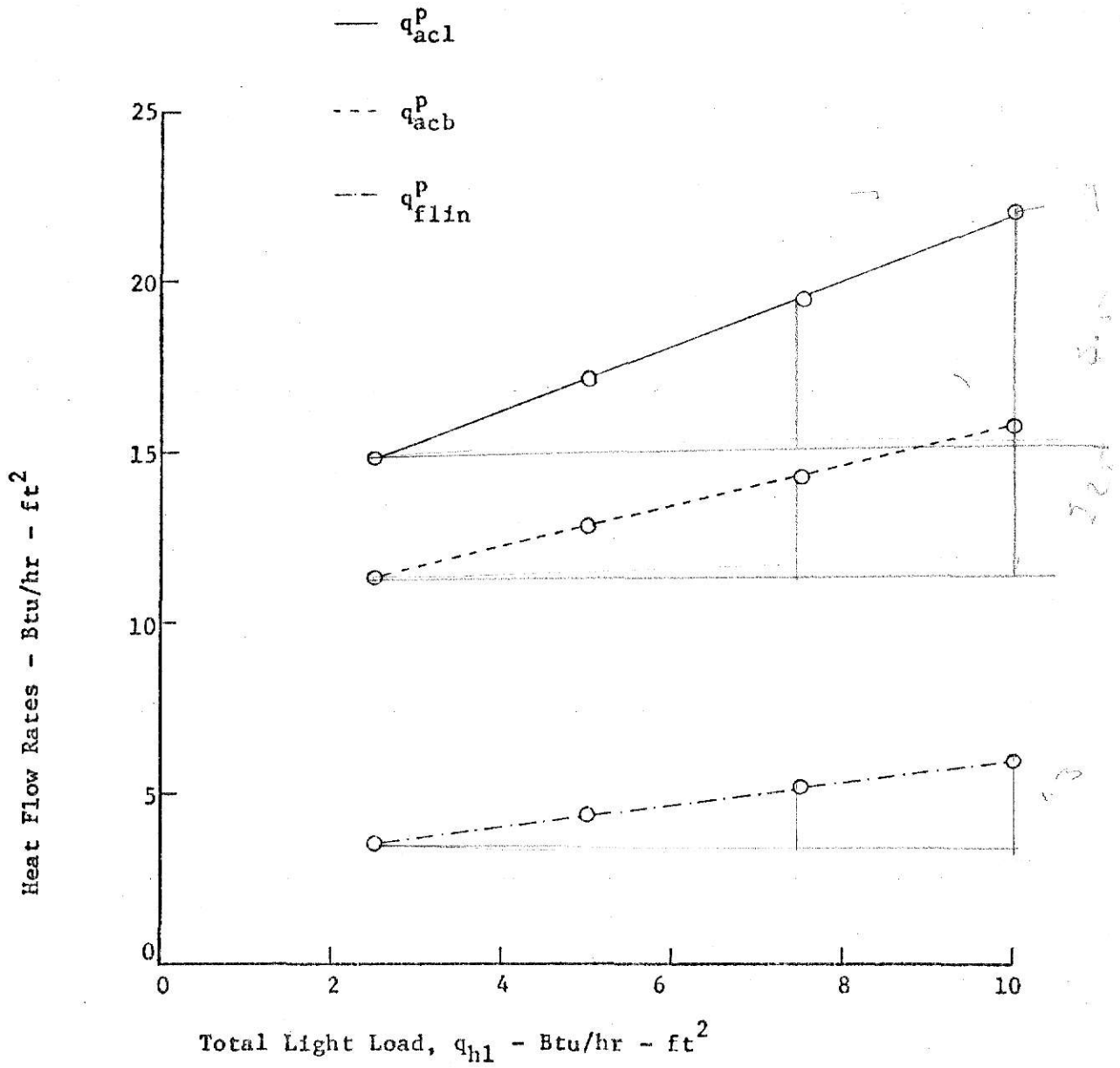


Figure 15. Effect of Varying the Light Load on the Peak Cooling Load.

Increasing the value of Q_{hl} while q_{hl} = constant raises the value of R as shown by equation (32),

$$R = \left(\frac{Q_{hl}}{\pi q_{hl}} \right)^{1/2} \quad (32)$$

This corresponds to having the same lighting load but fewer light fixtures. A variation over the range of 100 to 650 watts/fixture, produced no change in the computed air conditioning load, temperature profiles or any other variable.

Before increasing the distance between the light fixtures and the ceiling the validity of the assumption that the rising plume elements instantaneously spread uniformly across the top of the plume layer needs examination. As mentioned previously, Baines and Turner (6) concluded that $H/R = 1$ was the largest value of the ratio for which their analysis was fully valid. In order to satisfy this criterion, the values $R = 11.86$ feet and 650 watts/fixture were used corresponding to the same value of q_{hl} in the comparison. Upon increasing the value of d_{lc} from 2 feet to 5 feet and again to 8 feet, only a very slight trend of lowering q_{acl}^p was observed. Note that with the identical light source used in each of these runs approximately the same mass flow entered the air conditioned space from the stratified layer each run. Since the stratified layer cannot store the rising plume mass, it is reasonable to assume that the same effect would occur even if the H/R criterion was not satisfied. It should be noted, however, that adequate ceiling height is needed in order to satisfy the basic assumptions of the model. The supply air diffusers and return air inlets must not interfere with the stratified layer between the light level and the ceiling.

By increasing the thickness of insulation in the roof the cooling

load of the factory was reduced as shown in Figure 16. Practically all of this decrease was a result of a lower radiation heat transfer rate between the ceiling and the floor which enters the air conditioning space through q_{flin}^p .

The effect of exhausting ventilation air through the stratified layer and out the roof was compared with ejecting the air through the air conditioning system, as was done in the comparison run. Figure 17 shows that the cooling of the outdoor air for ventilation results in a larger increase in load than the reduction realized by exhausting the air from the stratified layer. However, exhausting needed ventilation through the roof significantly reduced the cooling load. When the ventilation air flow of the comparison run, 0.2 cfm/ft^2 , was exhausted through the stratified layer a decrease of $3 \text{ Btu/hr} - \text{ft}^2$ of q_{ac1}^p or 12% of the total peak cooling load was obtained. Thus, the convective portion of the lighting load was subtracted from the peak cooling load.

A close inspection of the curve corresponding to the rejection of air through the roof, showed that its slope is increasing as the ventilation rate increases. Thus, the additional reduction of the peak cooling load obtained by exhausting more air through the stratified layer decreases with increasing air flow. (As expected, the downward air flow from the stratified layer into the cooled space was not reversed until the exhausted air flow was increased to 0.2 cfm/ft^2 . For greater air flows the additional savings were considerably less because the radiation heat transfer from the ceiling can be reduced only slightly.

The sufficient air flows exhausted through the stratified layer which reduce the air conditioning load by the convective portion of the lighting

load are shown in Figure 18. Different outside air conditions would alter the curves in Figure 17 and 18 but the relationship between the two curves would be unchanged. From other computer runs no significant changes in the sufficient air flows were obtained with different thicknesses of insulation in the roof and higher sol-air temperatures. Thus, this occurrence depends only on the internal convective lighting load. The sufficient air flows are strongly dependent on the temperature of the lighting source since any change in the volume flux of the plume effects the downward air flow from the stratified layer into the cooled space.

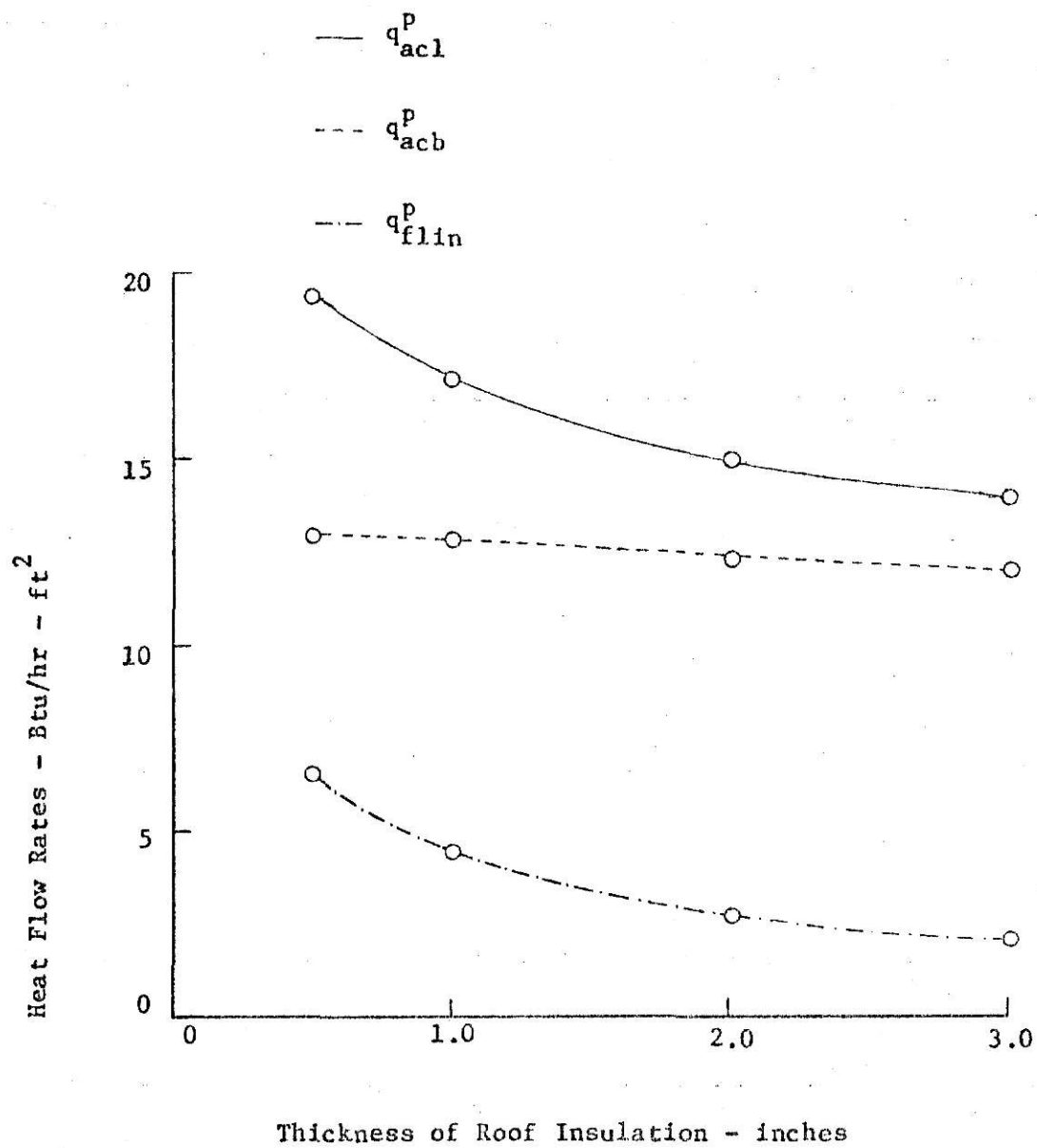


Figure 16. Effects of Varying the Thickness of Roof Insulation.

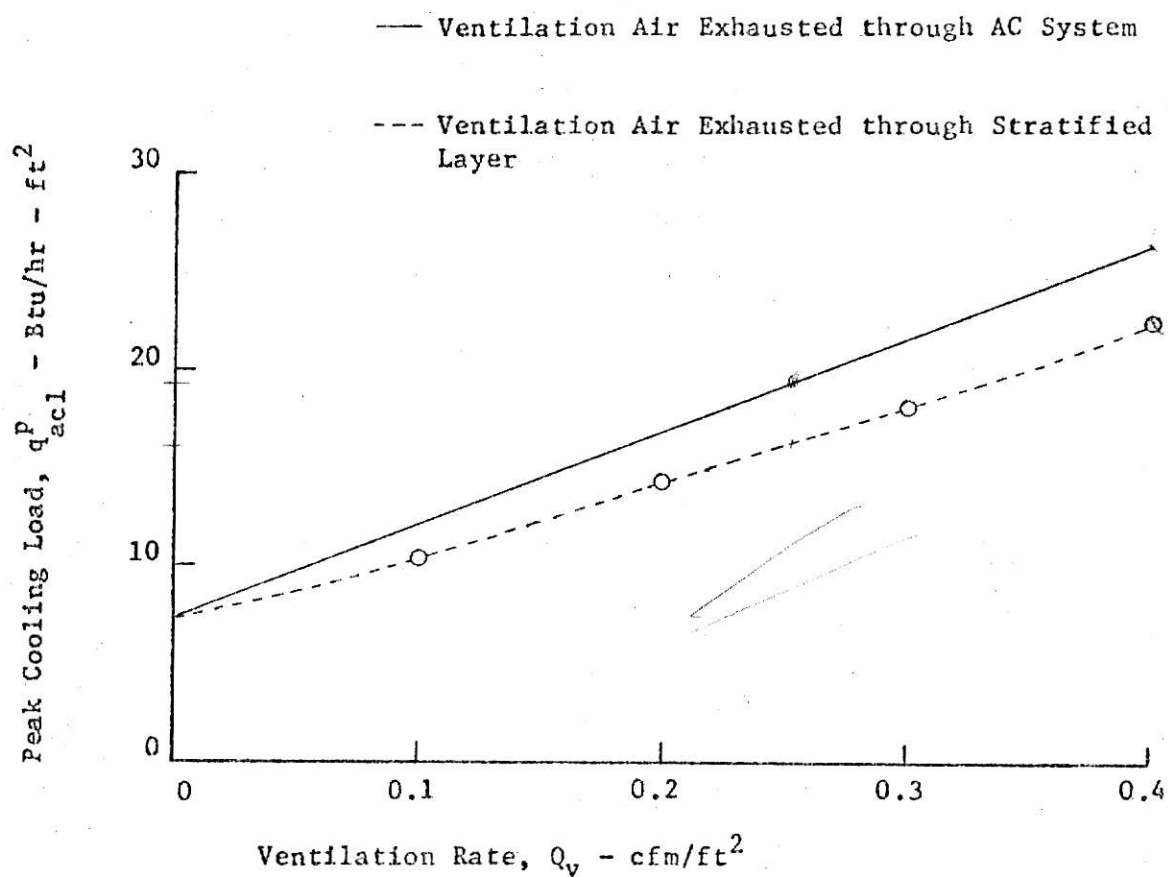


Figure 17. Comparison of the Peak Cooling Load With and Without Exhausting Ventilation Air through the Stratified Layer.

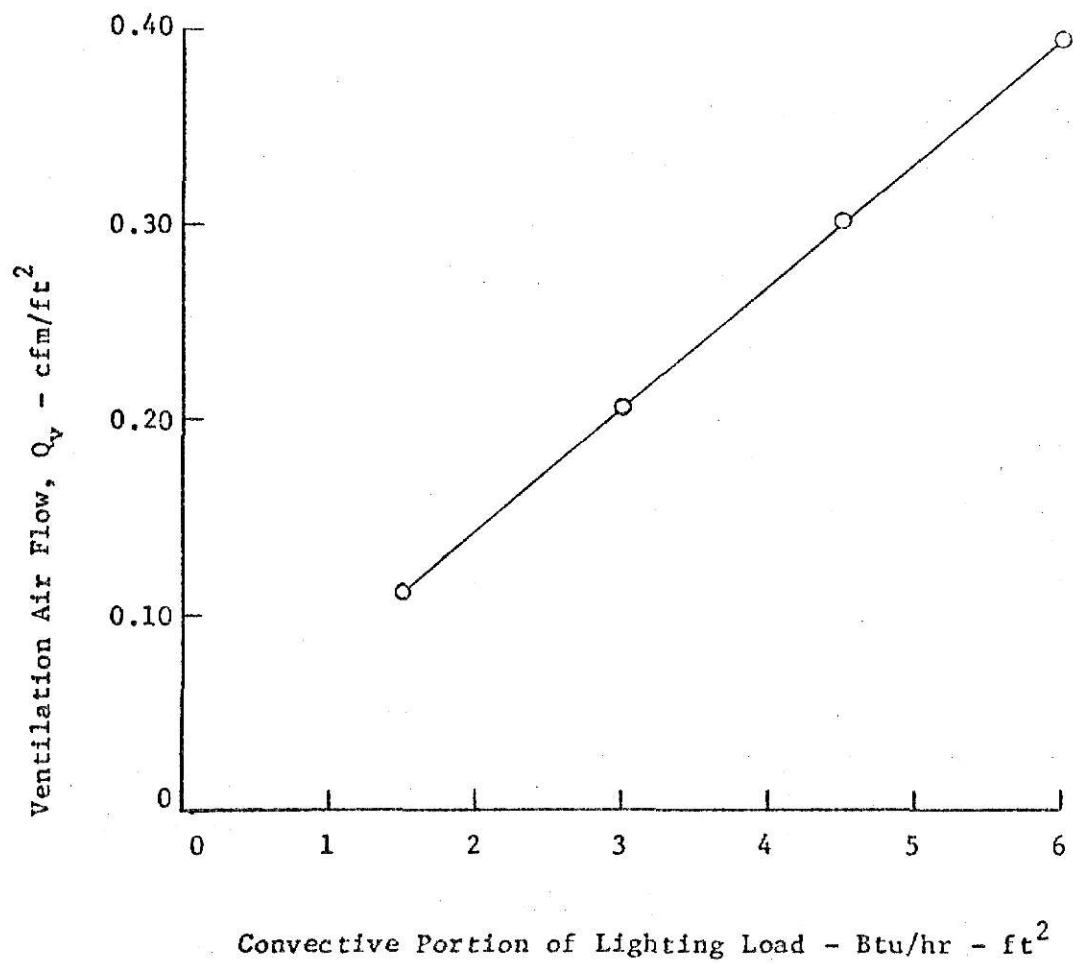


Figure 18. Sufficient Air Flows Exhausted through the Stratified Layer which Reduce the Cooling Load by the Convective Portion of the Lighting Load.

CHAPTER VII

SUMMARY AND CONCLUSIONS

This study has produced a numerical solution to the process of transient thermal stratification occurring in factories with high ceilings. The analysis was restricted by considering the light fixtures as the only internal sources which affect the stratification process. The solution was based on a simplified, physical model with thermal plumes rising from the light fixtures in a stratified layer between the level of the lights and the ceiling.

The results and discussion offer the designer of air conditioning systems some useful information about the thermal stratification. A summary of the relevant results is given below:

1. From the comparison with actual plant data the numerical solution approximately describes the thermal stratification process.
2. Without exhausting any ventilation air through the stratified layer convection heat transfer at the ceiling is practically eliminated and only radiation is important. At the time of peak load nearly all of the convective light load enters the air conditioning load. At other times a fraction remains in the stratified layer.
3. If the assumptions of the physical model are satisfied, varying the distance between the ceiling and the light fixtures does not significantly alter the air conditioning load..

4. Exhausting needed ventilation through the roof can reduce the cooling load by decreasing the convective portion of the light load which enters the air conditioned space. The sufficient air flows necessary to neglect the entire convective light load were obtained but they are strongly dependent on the temperature of the light fixtures.

CHAPTER VIII

RECOMMENDATIONS

Further verification of the results is required before applications can be handled with full confidence. A laboratory study in which the variables of the model could be accurately measured and varied is needed. Also, additional comparisons with actual factory cases would provide increased confirmation of both a laboratory study and the model.

Heat sources at the floor which affect the stratification process were completely neglected in this investigation. A study of rising, warmer air from concentrated sources in the air conditioned space would be much more complicated because the effects of turbulence in the cooled space must be included. In the present study the surrounding air of the plumes in the stratified layer was considered non-turbulent and no loss of buoyant fluid to this environment was assumed. However, in the turbulent cooled space some removal of fluid from the rising currents by the environment takes place in addition to the entrainment process. Also, the air diffusers may disturb the rising plumes and this would complicate the problem even more. Further study of the stratification process with these complications is needed before a full understanding can be obtained.

LIST OF REFERENCES

1. Dean, F. R. and Reese, J. A., "A New Approach to Factory Air Conditioning", Heating, Piping, and Air Conditioning, June, 1974, pp. 45-49.
2. Private Communication, Frank R. Dean Jr., Tempmaster Corporation, April 29, 1976.
3. Dralle, W. F., "Vertically Zoned Air Conditioning for High Ceiling Industrial Plants", Heating, Piping and Air Conditioning, December, 1970, pp. 69-72.
4. Olivieri, J. B., "A Consultant Looks at Complaints About Unitary A/C for Industrial Applications", Air Conditioning, Heating and Refrigeration News, February 4, 1974.
5. Morton, B. R., Taylor, G. I., and Turner, J. S., "Turbulent Gravitational Convection from Maintained and Instantaneous Sources", Royal Society of London, Proceedings, January, 1956, A 234, pp. 1-23.
6. Baines, W. D. and Turner, J. S., "Turbulent Buoyant Convection from a Source in a Confined Region", Jour. of Fluid Mechanics, 1969, Vol. 37, pp. 51-80.
7. Turner, J. S., "Buoyant Plumes and Thermals", Annual Review of Fluid Mechanics, Sears, W. R. and Van Dyke, M. Editors, Annual Reviews, Inc., Palo Alto, Calif., Vol. 1, 1969, pp. 29-44.
8. Barakat, H. Z. and Clark, J. A., "Analytical and Experimental Study of the Transient Laminar Natural Convection Flows in Partially Filled Liquid Containers", Proceedings of the Third International Heat Transfer Conference, Vol. II (1966), pp. 152-162.
9. Winter, E. R. F. and Schoenhals, R. J., "Analytical and Experimental Studies of Thermal Stratification Phenomena", Final Report, Part V, Heat Transfer Laboratory, Purdue University, (To NASA), October, 1968.
10. Dake, M. K. And Harleman, R. F., "Thermal Stratification in Lakes, Analytical and Laboratory Studies", Water Resources Research, Vol. 5, April 1969, pp. 484-495.
11. Armaly, B. F. and Lepper, S. P., "Diurnal Stratification of Deep Water Impoundments", ASME Publication, 75-HT-35.
12. ASHRAE Handbook of Fundamentals, American Society of Heating, Refrigerating and Air-Conditioning Engineers, Inc., New York, N. Y., 1972.

13. Isaacson, E. and Keller, H. B., Analysis of Numerical Methods, John Wiley and Sons, Inc., New York, 1966, pp. 85-99.
14. Clausing, A. M., "Numerical Methods in Heat Transfer", Advanced Heat Transfer, Edited by Chao, B. T. and Chato, J. C., Univ. of Illinois, 1967, pp. 238-332.
15. Crandall, S. H., Engineering Analysis, McGraw-Hill Book Co., New York, 1956, pp. 376-396.
16. Kreith, F., Principles of Heat Transfer, Second Edition, International Textbook Company, Scranton, Pa., 1969.

APPENDIX

Appendix A

Integration Over Plume Section With Gaussian Profiles

The character of a plume source depends only on the buoyancy flux and volume flux it provides. To determine an equivalent virtual source equations (36a) and (36b) were equated to the buoyancy flux and volume flux of the actual source. A derivation of these expressions of the buoyancy and volume flux of the virtual sources assuming the velocity and density profiles are Gaussian follows.

As a simple illustration assume that the velocity and density are constant across the plume and are zero outside it. Then,

$$\text{Volume flux} = \pi r_p^2 \bar{w} \quad (78a)$$

$$\text{Buoyancy flux} = \pi r_p^2 \bar{w} g (\rho_o - \rho_p) / \rho_r \quad (78b)$$

Now consider velocity and density profiles which are normal distribution curves centered about the axis of symmetry. Thus,

$$\bar{w}(z, r) = w(z) \exp(-r^2/b^2) \quad (2)$$

$$\bar{\Delta}(z, r) = g(\rho_o(z) - \rho(z, r)) / \rho_l = \Delta(z) \exp(-r^2/b^2) \quad (3)$$

For this case equations (78a) and (78b) become

$$\text{Volume flux} = \int_0^{2\pi} \int_0^\infty \bar{w}(z, r) r dr d\theta \quad (79a)$$

$$\text{Buoyancy flux} = \int_0^{2\pi} \int_0^\infty \bar{w}(z, r) \bar{\Delta}(z, r) r dr d\theta \quad (79b)$$

where integration is performed over a circular horizontal section of the plume.

The integration of (79a) and (79b) was completed as follows. Substitution of (2) into (79a) and integration yields

$$\begin{aligned} \text{Volume flux} &= \int_0^{2\pi} \int_0^\infty w(z) \exp(-r^2/b^2) r dr d\theta \\ &= 2\pi w(z) \int_0^\infty \exp(-r^2/b^2) r dr \\ &= \pi w(z) b^2(z) \int_0^\infty \exp(-r^2/b^2) d(r^2/b^2) \\ &= -\pi w(z) b^2(z) (0 - 1) \\ &= \pi w(z) b^2(z) \end{aligned} \quad (36a)$$

Similarly, substitution of (2) and (3) into (79b) and integration gives

$$\begin{aligned} \text{Buoyancy flux} &= \int_0^{2\pi} \int_0^\infty w(z) \exp(-r^2/b^2) \Delta(z) \exp(-r^2/b^2) r dr d\theta \\ &= 2\pi w(z) \Delta(z) \int_0^\infty \exp(-2r^2/b^2) r dr \\ &= \frac{\pi}{2} w(z) \Delta(z) b^2(z) \int_0^\infty \exp(-2r^2/b^2) d(2r^2/b^2) \\ &= \frac{\pi}{2} w(z) \Delta(z) b^2(z) \end{aligned} \quad (36b)$$

Thus, equations (36a) and (37b) are obtained.

A relationship between the bulk temperature and the axial temperature in the plume was desired. From the definition of bulk temperature,

$$\beta(T_b - T_{oal}) = \frac{\int_0^{2\pi} \int_0^{\infty} \bar{w}(z) \beta (T - T_o) r dr d\theta}{\int_0^{2\pi} \int_0^{\infty} \bar{w}(z) r dr d\theta}$$

From the previous integration it is obvious that

$$\beta(T_b - T_{oal}) = 1/2 \beta (T_m - T_{oal}) \quad . \quad (37)$$

Appendix B

Finite Difference Equations

The vertical space of the factory was partitioned into nodes of unit, horizontal area and implicit difference or nodal equations were derived by applying a heat balance to each node. Figure 19 shows the final arrangement of nodes with tolerable discretization errors in the comparison solution.

The fluid velocity in the stratified layer is expressed by

$$U_{pl}(\xi) = 3600 (V + U_s(\xi)) \quad (45)$$

$$U_{sl}(\xi) = 3600 V \quad (46)$$

These equations are evaluated at the boundaries of the nodes and the downward and upward hourly mass flows are represented by

$$\dot{m}_d^i = -\rho_a U_{pl}(\xi^i) \quad ; \quad \dot{m}_u^i = 0 \quad , \quad \text{if } U_{pl}(\xi^i) \leq 0 \quad (81a)$$

$$\dot{m}_u^i = \rho_a U_{pl}(\xi^i) \quad ; \quad \dot{m}_d^i = 0 \quad , \quad \text{if } U_{pl}(\xi^i) > 0 \quad (81b)$$

where $\xi^i = (d_s + (i-1) y_s) / H$, $i = 1, 2, \dots, N-8$ and $0 \leq \xi^i \leq 1$.

Different terms are needed since the temperature of a mass flow is dependent on its direction. Also, it is convenient to express the hourly mass flows of the plume motion before the superposition of the ventilation air flow as

$$\dot{m}_{pl}^i = 3600 \rho_a U_s(\xi^i) \quad (82)$$

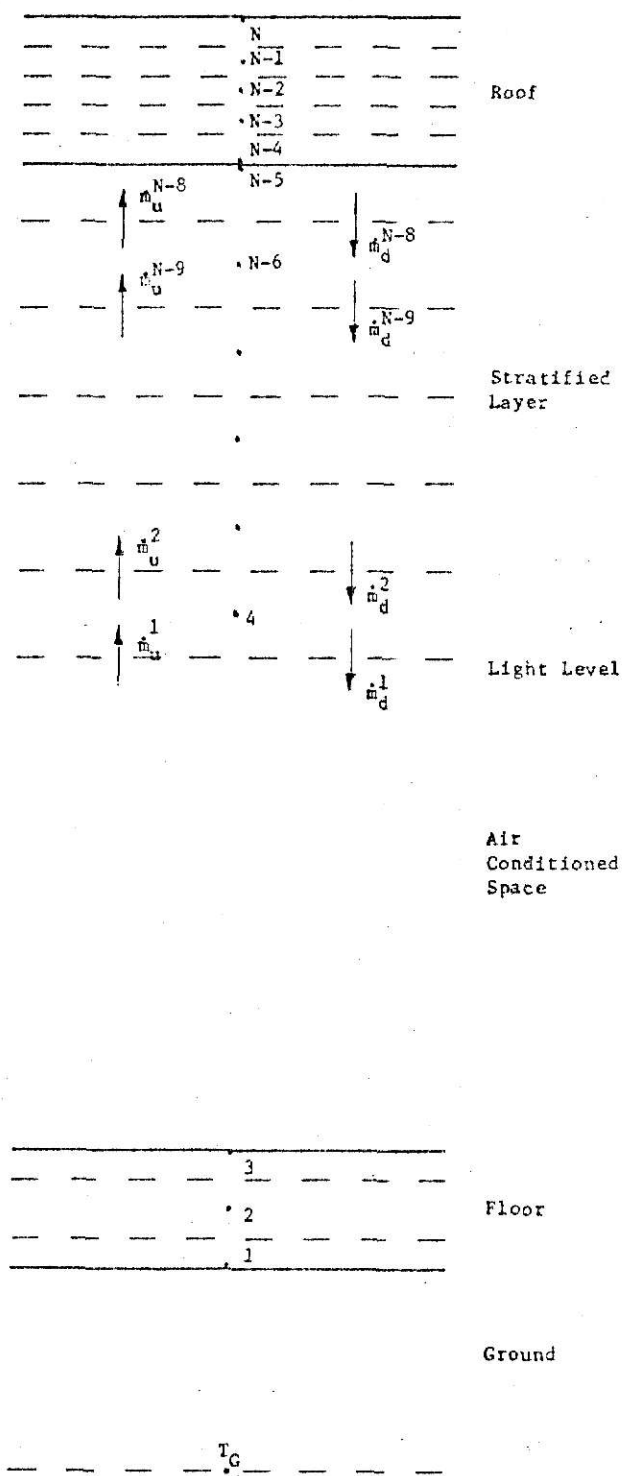


Figure 19. Arrangement of Finite Difference Nodes.

In the stagnant layer the mass flows are

$$\dot{m}_u^1 = 3600 \rho_a V ; \quad \dot{m}_d^1 = 0 \quad (83)$$

where $1 < \xi^1$.

A complete listing of the nodal equations using the numbering system in Figure 19 for the case of no stagnant layer is given below. The entrained air from each of the lower nodes in the plume layer is represented in the nodal equation of node N-5 since the plume carries the entrained air and delivers it to the top node of the plume layer. Thus, modification of the nodal equations for each thickness of the plume layer is necessary. For the details of these changes the computer program listed in Appendix C must be examined.

In the nodal equations the superscript denotes the time step and the subscript indicates the node which the temperature represents, T_1^t . A description and the thickness of each node is given in Table 2. The proper nodal equations are

$$\left[1 + \frac{2 \Delta t}{\rho_f c_f y_f} \left(c_g + \frac{k_f}{y_f} \right) \right] T_1^{t+1} = T_1^t + \frac{2 \Delta t C_g}{\rho_f c_f y_f} T_g^{t+1} + \frac{2 \Delta t}{\rho_f c_f y_f^2} T_2^{t+1} \quad (84)$$

$$\left[1 + \frac{2 \Delta t k_f}{\rho_f c_f y_f^2} \right] T_2^{t+1} = T_2^t + \frac{\Delta t k_f}{\rho_f c_f y_f^2} T_1^{t+1} + \frac{\Delta t k_f}{\rho_f c_f y_f^2} T_3^{t+1} \quad (85)$$

$$\left[1 + \frac{2\Delta t (k_f/y_f + h_f + h_r)}{\rho_f c_f y_f} \right] T_3^{t+1} = T_3^t + \frac{2\Delta t k_f}{\rho_f c_f y_f^2} T_2^{t+1} + \frac{2\Delta t h_f}{\rho_f c_f y_f} T_{ac} + \frac{F_{st} q_{hl}}{\rho_f c_f y_f} \quad (86)$$

$$\left[1 + \frac{\Delta t (3 k_a/y_s + (\dot{m}_d^2 + \dot{m}_u^1) c_a)}{\rho_a c_a y_s} \right] T_4^{t+1} = T_4^t + \frac{\Delta t (2 k_a/y_s + \dot{m}_u^1 c_a)}{\rho_a c_a y_s} T_{ac} + \frac{\Delta t (k_a/y_s + \dot{m}_d^2 c_a)}{\rho_a c_a y_s} T_5^{t+1} \quad (87)$$

$$\left[1 + \frac{\Delta t (2 k_a/y_s + (\dot{m}_d^{i-2} + \dot{m}_u^{i-3}) c_a)}{\rho_a c_a y_s} \right] T_i^{t+1} = T_i^t + \frac{\Delta t (k_a/y_s + \dot{m}_u^{i-3} c_a)}{\rho_a c_a y_s} T_{i-1}^{t+1} + \frac{\Delta t (k_a/y_s + \dot{m}_d^{i-2} c_a)}{\rho_a c_a y_s} T_{i+1}^{t+1}$$

$$i = 5, 6, \dots, N-7 \quad (88)$$

$$\left[1 + \frac{\Delta t (2 k_a/y_s + (\dot{m}_d^{N-8} + \dot{m}_u^{N-9}) c_a)}{CC} \right] T_{N-6}^{t+1} = T_{N-6}^t + \frac{\Delta t (k_a/y_s + \dot{m}_u^{N-9} c_a)}{CC} T_{N-7}^{t+1} + \frac{\Delta t (k_a/y_s + \dot{m}_d^{N-8} c_a)}{CC} T_{N-5}^{t+1} \quad (89)$$

$$CC = (\rho_{st} c_{st} F_{st} + \rho_a c_a (1 - F_{st})) y_s$$

TABLE 2

Description and Thickness of Nodes

| Node Number | Description | Thickness | Nodal Equation Number |
|-------------|--|-----------|-----------------------|
| 1 | Lower floor | $1/2 y_f$ | 84 |
| 2 | Middle floor | y_f | 85 |
| 3 | Top floor | $1/2 y_f$ | 86 |
| 4 | Lower stratified layer | y_s | 87 |
| 5 to N-7 | Middle stratified layer | y_s | 88 |
| N-6 | Stratified layer with structural steel | y_s | 89 |
| N-5 | Top stratified layer with structural steel | $1/2 y_s$ | 90 |
| N-4 | Ceiling or lower roof | y_1 | 91 |
| N-3 | Middle roof | y_2 | 92 |
| N-2 | Middle roof | y_2 | 93 |
| N-1 | Middle roof | y_2 | 94 |
| N | Top | y_3 | 95 |

$$\begin{aligned}
& \left[1 + \frac{2 \Delta t (k_a/y_s + h_c + (\dot{m}_d^{N-8} + 3600 \rho_a V) c_a)}{CC} \right] T_{N-5}^{t+1} \\
& = T_{N-5}^t + \frac{2 \Delta t (k_a/y_s + \dot{m}_u^{N-8} c_a)}{CC} T_{N-6}^{t+1} + \frac{2 \Delta t h_c}{CC} T_{N-4}^{t+1} \\
& + \frac{2 \Delta t c_a}{CC} \left[\dot{m}_{p1}^1 T_{ac} + (\dot{m}_{p1}^2 - \dot{m}_{p1}^1) T_4^{t+1} + (\dot{m}_{p1}^3 - \dot{m}_{p1}^2) T_5^{t+1} + \dots \right. \\
& \left. + (\dot{m}_{p1}^{N-8} - \dot{m}_{p1}^{N-9}) T_{N-6}^{t+1} \right] \quad (90)
\end{aligned}$$

$$\begin{aligned}
& \left[1 + \frac{\Delta t}{\rho_1 c_1 y_1} \left(\frac{1}{\frac{y_2}{2 k_2} + \frac{y_1}{k_1}} + h_c + h_r \right) \right] T_{N-4}^{t+1} \\
& = T_{N-4}^t + \frac{\Delta t h_c}{\rho_1 c_1 y_1} T_{N-5}^{t+1} + \frac{\Delta t h_r}{\rho_1 c_1 y_1} T_3^{t+1} + \frac{\Delta t}{\rho_1 c_1 y_1 \left(\frac{y_2}{2 k_2} + \frac{y_1}{k_1} \right)} T_{N-3}^{t+1} \\
& \quad (91)
\end{aligned}$$

$$\begin{aligned}
& \left[1 + \frac{\Delta t}{\rho_2 c_2 y_2} \left(\frac{1}{\frac{y_2}{2 k_2} + \frac{y_1}{k_1}} + \frac{k_2}{y_2} \right) \right] T_{N-3}^{t+1} \\
& = T_{N-3}^t + \frac{\Delta t}{\rho_2 c_2 y_2 \left(\frac{y_2}{2 k_2} + \frac{y_1}{k_1} \right)} T_{N-4}^{t+1} + \frac{\Delta t k_2}{\rho_2 c_2 y_2^2} T_{N-2}^{t+1} \quad (92)
\end{aligned}$$

$$\left[1 + \frac{2 \Delta t k_2}{\rho_2 c_2 y_2^2} \right] T_{N-2}^{t+1} = T_{N-2}^t + \frac{\Delta t k_2}{\rho_2 c_2 y_2^2} T_{N-1}^{t+1} + \frac{\Delta t k_2}{\rho_2 c_2 y_2^2} T_{N-3}^{t+1} \quad (93)$$

$$\left[1 + \frac{\Delta t}{\rho_2 c_2 y_2} \left(\frac{1}{\frac{y_2}{2 k_2} + \frac{y_3}{k_3}} + \frac{k_2}{y_2} \right) \right] T_{N-1}^{t+1} \\ = T_{N-1}^{t+1} + \frac{\Delta t k_2}{\rho_2 c_2 y_2^2} T_{N-2}^{t+1} + \frac{\Delta t}{\rho_2 c_2 y_2 \left(\frac{y_2}{2 k_2} + \frac{y_3}{k_3} \right)} T_N^{t+1} \quad (94)$$

$$\left[1 + \frac{\Delta t}{\rho_3 c_3 y_3} \left(\frac{1}{\frac{y_2}{2 k_2} + \frac{y_3}{k_3}} + h_s \right) \right] T_N^{t+1} \\ = T_N^t + \frac{\Delta t}{\rho_3 c_3 y_3 \left(\frac{y_2}{2 k_2} + \frac{y_3}{k_3} \right)} T_{N-1}^{t+1} + \frac{\Delta t h_s}{\rho_3 c_3 y_3} T_{sat}^{t+1} \quad (95)$$

If the air conditioning system, factory equipment and lights are turned off during a portion of the daily cycle, the desired temperature of the cooled space is no longer maintained. Since no plume motion exists, only conduction heat transfer occurs in the stratified layer. An extra difference equation to be solved for the changing temperature of the lower space was added to the above listing. The heat transfer through the factory walls is significant in determining the temperature of the lower space during this period. Thus, it is included in the difference equation for the lower space was written as:

$$\left[1 + \frac{\Delta t (U_w (\Lambda_w/\Lambda_f) + h_f + 2 k_a/y_s)}{\rho_a c_a y_{ac}} \right] T_{acc}^{t+1}$$

$$= T_{acc}^t + \frac{\Delta t h_f}{\rho_a c_a y_{ac}} T_3^{t+1} + \frac{2 \Delta t k_a/y_s}{\rho_a c_a y_{ac}} T_4^{t+1} + \frac{\Delta t U_w (\Lambda_w/\Lambda_f)}{\rho_a c_a y_{ac}} T_{oa}^{t+1} .$$

(96)

Appendix C

The computer program using the FORTRAN IV language is presented on the following pages.


```

C W(4,11)--AXIAL, VERTICAL VELOCITY OF THE PLUME--FT/SEC
C BELTIN THE DISTANCES ARE IN FT
C Y1--SPATIAL INCREMENT OF THE LOWER ROOF NODE
C Y2--SPATIAL INCREMENT OF THE MIDDLE ROOF NODES
C Y3--SPATIAL INCREMENT OF THE TOP ROOF NODE
C YS--SPATIAL INCREMENT OF THE NODES IN THE STRATIFIED LAYER
C YF--SPATIAL INCREMENT OF THE FLOOR NODES
C YAC--THICKNESS OF AC SPACE
C Z11--DIMENSIONLESS HEIGHT
C DIMENSION TC(14,15),TS(16),TN(16),G(33),SAT(48),TEMP(48,16)
C DIMENSION TPLUM(48,3),UMF(11),FMD(11),G(11),TDA(48)
C DIMENSION U(11),FM(11),Z(11),GMLJ(11),D(48),E(48),F(10)
C DIMENSION DMLK(11),DMLH(11),DMLL(11),N(48,6),R(48,6)
C DIMENSION QGOLF(48),QGSLL(48),QPAD(48),QPSL(48),QSR(48),QACR(48)
C DIMENSION QFLST(48),QGST(48),QFLUT(48),QFLUT(48),QACL(48)
C DIMENSION RPI(48,6),UMF(48,6),DME(48,6),RST(48),RFS(48),RNS(48)
C DIMENSION REAL(48),VECHER(48),VEAL(48),VFCHEK(48),QL(48),VF(48)
C DIMENSION VFI(48),FCI(15,16),TE(15),CIAC(4),TEMPAC(48)
C REAL K1,K2,K3,KA,KF
C NIN = 6
C MIN = MIN+3
C N = MIN+8
C N1 = N+1
C NPY = MIN+2
C M = 1
C MOEF = 23
C MOP = 31
C N11 = 46
C N11 = N1+1
C SAC = 0.1714E-8
C 101 FORMAT (9F10.5)
C 102 FORMAT (6F10.5)
C 103 FORMAT (7F10.5)
C 104 FORMAT (13F6.1)
C 105 FORMAT (13,3X,M,3X,MINS,6X,OS,10X,AFAS,8X,RFAL,7X,BECH
C X8,8X,VEAL,6X,VECHER,6X,TEMPAC,7X,TPAL,8X,QTOT,6X,QCHE
C X8,8X,VEAL,6X,VECHER,6X,TEMPAC,7X,TPAL,8X,QTOT,6X,QCHE
C X8,8X,VEAL,6X,VECHER,6X,TEMPAC,7X,TPAL,8X,QTOT,6X,QCHE
C 106 FORMAT (' ',14,15,9F12.6)
C 107 FORMAT ('1', THE CENTERLINE PLUME VELOCITY (FT/MIN), W(4,11) /)
C 108 FORMAT (' ',3X,M,7X, '1',10X, '2',10X, '3',10X, '4',10X, '5',10X,
C X8,8X,VEAL,6X,VECHER,6X,TEMPAC,7X,TPAL,8X,QTOT,6X,QCHE
C 109 FORMAT (' ',14, 6F11.2)
C 110 FORMAT ('1', PLUME RADIUS (FT), RPI(M,1) /)
C 111 FORMAT ('1', APPROX MASS FLOW RATES (LBS/HR), UMF(M,1) /)
C 112 FORMAT ('1', APPROX MASS FLOW RATES (LBS/HR), DME(M,1) /)
C 113 FORMAT ('1', PLUME TEMPERATURES (DEG F) TPLUM(M,1) /,3X,
C X8,8X,VEAL,6X,VECHER,6X,TEMPAC,7X,TPAL,8X,QTOT,6X,QCHE
C 114 FORMAT (14, 6F11.2)
C 115 FORMAT ('1', PLUME TEMPERATURES (DEG F), TEMP(M,1) /,3X, '4',6X,
C X1,7X, '2',7X, '3',7X, '4',7X, '5',7X, '6',7X, '7',7X, '8',7X, '9',7X, '10',
C X1,7X, '11',6X, '12',6X, '13',6X, '14' /)
C 116 FORMAT (14,14F8.1)
C 117 FORMAT ('1',2X,M,5X,QGOLF,6X,QGSLL,7X,QPAD,7X,QPSL,8X,
C X1,7X, '2',7X, '3',7X, '4',7X, '5',7X, '6',7X, '7',7X, '8',7X, '9',7X, '10',
C X1,7X, '11',6X, '12',6X, '13',6X, '14' /)
C 118 FORMAT (14,11F11.2)
C 119 FORMAT ('1',7X, '2',7X, '3',7X, '4',7X, '5',7X, '6',7X, '7',7X, '8',7X, '9',7X, '10',
C X1,7X, '11',6X, '12',6X, '13',6X, '14' /)
C 120 FORMAT (6F10.6)

```

```

43 READ(5,120) VL,Y2,Y3,YS,YF,VAC
44 READ(5,102) DL,D2,D3,D4,DF,DST
45 READ(5,102) SH1,SH2,SH3,SHA,SHE,SHST
46 READ(5,101) KL,K2,K3,K4,KF,EMC,EMF,CG
47 READ(5,104) HS,HF,QLITS,II,EST,FRL,TEMPG
48 READ(5,104) (SAT(I),I=1,12)
49 READ(5,104) (SAT(I),I=13,24)
50 READ(5,103) DUC,P,FC,TAC,TDM,VEN,VENS
51 READ(5,104) (IOA(I),I=1,12)
52 READ(5,104) (IOA(I),I=13,24)
53 TAC = TAC*460.0
54 DO 1 I=1,N
55 1 TQ(I) = YS*0
56 DO 57 I=1,NIN
57 57 QFM(I) = 0.0
58 DO 2 I=1,24
59 2 TQA(I*24) = IOA(I)
60 2 SAT(I*24) = SAT(I)
61 DO 82 I=1,NQFF
62 82 QLITS = QLITS
63 VF(I) = 61.0*DA*VEN
64 V(I) = 60.0*DA*VENS
65 MDEF1 = MDEF+1
66 4041 = MDEF-1
67 DO 87 I=MDEF1,MCON1
68 87 V(I) = 0.0
69 VF(I) = 0.0
70 V(I) = 0.0
71 DO 88 I=MOA,48
72 88 VF(I) = 60.0*DA*VEN
73 QLITS = QLITS
74 V(I) = 60.0*DA*VENS
75 MINS = MIN
76 VFS = NIN+3
77 MPIS = MPN
78 S = QLC
79 FMS = (1.0/EMC)*(1.0/EMF)-1.0
80 C(1) = 1.0*(2.0*(11/(DF*SH*YF)))*(CG+(KF/YF)))
81 C(2) = 1.0*(2.0*(TICK)/(YF*YF*DF*SH*YF))
82 C(5) = 11*SF/(CF*SH*YF*YF)
83 C(6) = 2*TI*KF/(CF*SH*YF*YF)
84 C(8) = 2*TI*KF/(DF*SH*YF*YF)
85 C(9) = 11*KF/(YF*YF*DF*SH*YF)
86 C(13) = 1.0*(11/(12*SH2*Y2))*11.0/(Y1/K1+Y2/(K2*2.0))*K2/(Y2))
87 C(19) = 1.0*(2.0*(TI*42/(12*SH2*Y2*Y2)))
88 C(23) = (11/(12*SH2*Y2))*11.0/(Y1/K1+Y2/(2*K2))
89 C(24) = 11*K2/(12*SH2*Y2*Y2)
90 C(27) = (11/(11*SF1*Y1))*1.0/(Y2/(2.0*K2)+Y1/K1))
91 C(28) = C(24)
92 C(29) = 2.0*TI*CF*TEMPG/(DF*SH*YF)
93 C(41) = C(24)
94 C(42) = 1.0*(11/(12*SH2*Y2))*11.0/(Y2/(2.0*K2))+Y3/K3)) +K2
95 X(Y2))
96 C(43) = 1.0*(11/(12*SH2*Y2))*11.0/(Y3/K3+Y2/(2.0*K2)))))
97 C(14) = C(24)
98 CR(5) = (11/(12*SH2*Y2))*11.0/(Y2/(2*K2))+Y3/K3))
99 CR(6) = (11/(12*SH2*Y2))*11.0/(Y2/(2*K2))+Y3/K3))
100 CQ2 = 2.0*K4/Y5
101 CQLIT = (1.0-FRL)*QL(M)/3600.0
102 PQLS = 3.1416*(R**2.0)*CQLIT

```

```

102 TPAL(M) = 0.5*(TPM-TO(4))*TO(4)
103 VFAL(M) = QLS/(DA*SHA*(TPAL(M)-TAC))
104 IF (MINS .GT. 3) GO TO 96
105 BFAL(M) = 0.0
106 GO TO 296
107 96 REFL(M) = VFAL(M)*32.2*(TPAL(M)-TO(4))/TAAC
108 296 QAC = 0.0
109 DO 55 I=1,MIN
110 55 QFM(I) = 0.0
111 IF (REFL(M) .GT. 0.0) GO TO 95
112 GO TO 31
113 95 DS(M) = ((0.253*VFAL(M))*0.6)*((1.0/EC)**0.3)*((1.0/BFAL(M))*0.2
X)
114 C1 = 64.0*(13.1416*EC*EC/VFAL(M))*2.0)*32.174*(TPAL(M)-TO(4))/(T
XAC=S)
DO 50 I=1,20
115 50 V1 = DS(M)/(DS(M)+S)
116 V2 = (V1*(5.0/3.0)) + (0.452*V1*(-0.0583-0.01*V1))
117 V3 = V2*3.0
118 V4 = (V1*(2.0/3.0)) + (0.765*V1*(-0.157-0.0367*V1))
119 FDS = (C1*(S+DS(M))*6.0)*V3)-1.0
120 DFOS = C1*((6.0*(S+DS(M))*5.0)*V3)+(S*((S+DS(M))*4.0)*V2-V2*V4
X)-3.3)
121 95AV = DS(M)
122 DS(M) = DS(M)-(FDS/DFOS)
123 CVG = ARS(OSAV-DS(M))
124 IF (CVG .LT. 0.01) GO TO 81
125 80 CONTINUE
126 81 BEAS(M) = ((S+DS(M))/S)*BFAL(M)
127 H = DS(M)+S
128 Z(I) = DS(M)/H
DO 10 I=1,MINS
129 10 Z(I) = ((1-I)*VS+DS(M))/H
DO 11 I=1,MINS
130 11 DIMLJ(I) = 0.459*(Z(I)*(5./3.))-0.0588*(Z(I)*(8./3.))-0.01*(Z(I)
X*(11./3.))
DO 3 I=1,MINS
131 3 DIMLX(I) = 0.765*(Z(I)*(2./3.))-0.157*(Z(I)*(5./3.))-0.0366*(Z(I)
X*(8./3.))
132 DIMLX(I) = DIMLJ(I)/DIMLX(I)
133 DIMLX(I) = DIMLX(I)/DIMLX(I)
DO 4 I=1,MINS
134 4 M(I) = ((BEAS(M)/(3.1416*H*(EC**2.0)))*V*(1.0/3.0))*DIMLX(I)*60.0
3(M,I) = 2.0*FC*H*DIMLX(I)
135 5P(M,I) = 2.144*H*H,I)
DIMLF = ((1.0-7(I))/DIMLJ(I))
136 5FC*H(M) = 0.5*((((H*FAS(M)/3.1416)**2.0)*(1.0/(EC**4.0)))*(1.0/(H*
X*5.0)))*((1.0/3.0))*DIMLF*3.1416*0.5*H(M,I)*(8(M,I)**2.0)/60.0
IF (MINS .EQ. MIN) GO TO 7
137 MVS1 = MVS+1
DO 8 I=MINS1,MIN
138 8 Z(I) = 0.0
X(I) = 0.0
139 8 5P(M,I) = 0.0
DO 12 I=1,MINS
140 12 J(I) = 4.41*(BEAS(M)/(3.1416*H))*((1./3.))*V*(EC**4./3.))*((H/R)**2.
X)*DIMLJ(I)
141 5FC*H(M) = U(I)*3.1416*(R**2.)
DO 13 I=1,MINS
142 13 FM(I) = DAWU(I)*3600.0

```



```

155 IF (NINS.EQ.NIN) GO TO 43
156 NINS1 = NINS+1
157 DO 60 I=NINS1,NIN
158   UFM(I) = V(M)
159   FM(I) = 0.0
160   43 07 55 I=1,NIN
161   55 FXP(I) = FM(I)
162   IF (V(M).EQ. 0.0) GO TO 39
163   NI = NINS+1
164   DO 50 I=1,NINS
165     FM(NI-I) = FM(NI-1)-V(M)
166     DO 58 I=1,NINS
167       VS = I
168       IF (FM(NI-I) .LT. 0.0) GO TO 51
169     58 CONTINUE
170     GO TO 39
171     51 00 53 I=NS,NINS
172     53 UFM(NI-I) = -FM(NI-1)
173     DO 54 I=NS,NINS
174       FM(NI-I) = 0.0
175     IS = NI-NS
176     GO TO 39
177     21 00 32 I=1,NIN
178     FXP(I) = 0.0
179     UFM(I) = V(M)
180     FP(M,1) = 0.0
181     M(1,1) = 0.0
182     TPLM(M,1+2) = 0.0
183     32 FM(I) = 0.0
184     DS(M) = 0.0
185     SEASON(M) = 0.0
186     BFCHEK(M) = 0.0
187     VFCHEK(M) = 0.0
188     QUAC = (1.0-FQL)*QL(M)*TI
189     C(4) = 1.0+TI*(1.0-(KA/YS))*(FM(2)+UFM(1))*SHA)/(DA*SHA*YS))
190     C(11) = TI*(KA/YS+FM(2)*SHA)/(DA*SHA*YS)
191     C(12) = UFM(1)*TAC
192     CC = (DST*SMST+FST+DA*SHA*(1.0-FST))*YS
193     C(15) = 1.0+TI*(2.0*(KA/YS)*(FM(N-8)+UFM(N-9))*SHA)/(CC)
194     C(20) = TI*(KA/YS+UFM(N-9)*SHA)/CC
195     C(21) = 2.0*TI*((KA/YS)+UFM(N-3)*SHA)/CC
196     C(25) = TI*((KA/YS)+FM(N-8)*SHA)/((DST*SMST+FST+DA*SHA*(1.0-FST))*
      XYS)
197     VS = N-7
198     DO 15 I=5,NS
199       C(1-4) = 1.0+TI*(2.0*(KA/YS)*(FM(1-2)+UFM(1-3))*SHA)/(DA*SHA*YS))
200       C(1-4) = TI*((KA/YS)+UFM(1-3)*SHA)/(DA*SHA*YS)
201       15 C(1-4) = TI*(KA/YS+FM(1-2)*SHA)/(DA*SHA*YS)
202       31FM = MINS+1-MIN
203       IF (31FM 7)-68,69
204       69 C(15) = 1.0+TI*(2.0*(KA/YS)*(FM(N-9)+V(M))*SHA)/(CC)
205       GO TO 69
206       70 YSCH = MINS-4
207       IF (YSCH .LT. 1) GO TO 269
208       31MINS-4) = 1.0*TI*(2.0*(KA/YS)*(FM(MINS-3)+V(M))*SHA)/(DA*SHA*YS))
209       GO TO 69
210       269 C(4) = 1.0*(TI*(3.0*(KA/YS)*(FM(1)+UFM(2))*SHA)/(DA*SHA*YS))
211       69 DUTC = FXP(1)*SHA*TPAL(4)
212       CONST = 2.0*TI/((DST*SMST+FST+DA*SHA*(1.0-FST))*YS)
213       IF (MINS+1-MIN) 61,62,63

```

```

214 61 CONST = 1/4 (DA*SHA*YS)
215 GO TO 63
216 62 CONST = 0.5*CONST
217 DO 14 I=5,MINS
218 14 F(I-4) = CONST*(FMP(I-3)-FMP(I-4))*SHA
219 C(32) = CONST*OLTC
220 TRA = TC(N-4)+60.0
221 TEA = TC(3)+460.0
222 IF (TEA-TEA) 16,17,16
223 17 HZ = 0.0
224 GO TO 18
225 16 HZ = SBCP(TEA*4.-TEA*4.)/((TRA-TEA)*EME)
226 18 HC = 1.08
227 HZP = TC(N-4)-TC(N-5)
228 IF (HZP) LT,0.0) HC=1.68
229 IF (HYS - FQ. MIN) HC=1.68
230 C(3) = 1.0*((12-TJ)*(YF+H*YF+H*H*YF)/(DF*SHF*YF*YF))
231 C(13) = 2*TI*H2/(DF*SHF*YF)
232 C(14) = TI*H2/(DI*SHI*YI)
233 C(16) = 1.0*((12.0-TJ)*(KA*YS+HC*(FM(N-8)*V(M))*SHA))/CC)
234 C(17) = 1.0*(TI*(DI*SHI*YI))*11.0/(Y2/(2*H2)+V1/K1+HC+HR)
235 C(22) = TI*H2/(DI*SHI*YI)
236 C(26) = 2.0*TI*HC/(DI*SHI*YI)
237 C(33) = TI*H2*SAT(W)/DI3*SHI*YI
238 IF (M - GT. MOFF) GO TO 72
239 GO TO 73
240 72 IF (H - LT. HCN) GO TO 74
241 73 C(30) = 2.0*FRL*TI*OL(M)/(DF*SHF*YF)+2.0*TI*H*F*TAC/(DF*SHF*YF)
242 C(7) = 0.0
243 C(10) = 0.0
244 C(31) = TI*(2*(KA/YS)*UFM(1)-SHA)*TAC/(CA*SHA*YS)
245 201 DO 22 I=1,N
246 DO 21 J=1,M1
247 TC(I,J) = 0.0
248 21 CONTINUE
249 22 CONTINUE
250 DO 23 I=1,4
251 TC(I,1) = C(1)
252 23 TC(I,1+1) = -C(1+7)
253 DO 24 I=2,4
254 TC(I,1-1) = -C(1+3)
255 TC(3,1-4) = -C(11)
256 TC(1-4,3) = -C(114)
257 K=4-7
258 DO 25 I=5,K
259 TC(I,1) = 0.0
260 TC(I,1-1) = -G(1-4)
261 25 TC(I,1+1) = -F(1-4)
262 11=0
263 FK = N-6
264 DO 26 I=KK,N
265 11 = 11+1
266 TC(I,1) = C(14+11)
267 26 TC(I,1-1) = -C(119+11)
268 11=0
269 KL = N-3
270 DO 27 I=KK,KL
271 11 = 11+1
272 27 TC(I,1+1) = -C(24+11)
273 TC(N-2,N-1) = -CH(1)

```

```

274 DO 301 I=1,2
275 TC(N-2+1,N-2+1) = CR(I+1)
276 301 TC(N-2+1,N-3+1) = -C8(I+1)
277 TC(N-1,N) = -C8(6)
278 JS = MINS-5
279 IF (JS.LT. 1) GO TO 87
280 DO 33 J=1,JS
281 33 TC(MINS,J+3) = -F(J)
282 89 MSCM = MINS-4
283 IF (MSCM.LT. 1) GO TO 280
284 TC(MINS,MINS-4+3) = TC(MINS,MINS-4+3)-F(MINS-4)
285 280 TC(1,N1) = T(1)+C(29)
286 TC(2,N1) = T(2)
287 DO 28 I=3,4
288 28 TC(I,N1) = T(I)+C(27+1)
289 DO 29 I=5,N
290 29 TC(I,N1) = T(I)
291 TC(MINS,N1) = TC(MINS,N1)+C(32)
292 TC(N,N1) = TC(N,N1)+C(33)
293 MCHK = 0.0
294 64 CALL GJELIM(TC,TN,N1,MINS)
295 GO TO 65
296 74 NO = N+1
297 NO1 = NO+1
298 DO 222 I=1,NO
299 DO 221 J=1,N01
300 FC(I,J) = 0.0
301 221 CONTINUE
302 222 CONTINUE
303 C(30) = 0.0
304 C(31) = 0.0
305 C(7) = 2.0*Y1*K4/(DA*SHA*YS*YS)
306 C(10) = 2.0*TIMEF/(DF*SHF*YF)
307 CTAC(1) = -TIMEF/(DA*SHA*YAC)
308 CTAC(2) = 1.0+(Y1*(H+2.0*(KA/Y51+0.2375)/(DA*SHA*YAC))
309 CTAC(3) = -2.0*Y1*K4/(DA*SHA*YAC*YS)
310 CTAC(4) = 0.2375*Y1*TDAIN/(DA*SHA*YAC)
311 GO1 = 0.0
312 DO 223 I=1,3
313 FC(I,1) = C(1)
314 223 FC(I,1+1) = -C(I+7)
315 DO 224 I=2,3
316 FC(I,1-1) = -C(I+3)
317 FC(3,N1-4) = -C(13)
318 FC(N1-4,3) = -C(14)
319 DO 220 I=1,3
320 FC(4,I+2) = CTAC(I)
321 FC(5,4) = -C(7)
322 FC(5,5) = C(4)
323 FC(5,6) = -C(11)
324 K = NS-7
325 DO 225 I=6,K
326 FC(I,1) = 0(1-5)
327 FC(1,1-1) = -G(1-5)
328 225 FC(I,1+1) = -F(1-5)
329 I1 = 0
330 KY = NJ-6
331 DO 226 I=KK,NO
332 I1 = I1+1
333 FC(I,1) = C(14+I1)

```

```

334 FC(I,I-1) = -C(I9+11)
335 IJ = 0
336 KL = NJ-3
337 DO 227 I=KK,KL
338   IJ = IJ+1
339   227 FC(I,I+1) = -C(24+IJ)
340   FC(NJ-2,NJ-1) = -C(1)
341   DO 302 I=1,2
342     FC(NJ-2+I,NJ-2+I) = C(I+1)
343   302 FC(NJ-2+I,NJ-3+I) = -C(I+3)
344   FC(NJ-1,NJ) = -C(16)
345   FC(I,NJ) = TO(I)*C(29)
346   DO 228 I=2,3
347     228 FC(I,NJ) = TO(I)
348     FC(I,NJ) = CTAC(4)+TEMPAC(M-1)
349   DO 229 I=5,NJ
350     229 FC(I,NJ) = TO(I-1)
351     FC(NJ,NJ) = FC(NJ,NJ)+C(33)
352     WHEN = 1
353   310 CALL GUELM(FC,TF,NJ,NJ,MINSO)
354   DO 230 I=1,3
355     TN(I) = TF(I)
356     TEMP(M,I) = TF(I)
357     TO(I) = TF(I)
358   DO 231 I=5,NJ
359     TN(I-1) = TF(I)
360     TEMP(M,I-1) = TF(I)
361     TO(I-1) = TF(I)
362     TEMPAC(M) = TF(4)
363     GO TO 38
364   65 DO 19 I=1,N
365     TEMP(M,I) = TN(I)
366   19 TO(I) = TN(I)
367   COL = EM(1)*TN(4)
368   TEMPAC(M) = TAC
369   IF (IPAL(M).GT. 0.0) GO TO 86
370   MINS = 4
371   MNS = 3
372   EMPUM = EMP(I)
373   QPLUM = EMP(I)*SHA*TPAL(M)
374   TPLUM(M,3) = TPAL(M)
375   MPCH = MNS-1
376   IF (MPCH.LT. 1) GO TO 290
377   DO 5 I=4,MNS
378     EMADN = EMP(I-2)-EMP(I-3)
379     EMPUM = EMADN+EMPUM
380     CPLUM = QPLUM+EMADN*SHA*TN(I)
381   5 TPLUM(M,I) = QPLUM/(EMPUM+SHA)
382   290 MPIS = MNS-MCH
383   IF (MPDIFF.FO. 0) GO TO 37
384   MPNSI = MNS+1
385   DO 6 I=MPNSI,MPN
386     6 TPLUM(M,I) = 0.0
387   37 MINSN = MINS
388   DO 35 I=4,MIN
389     35 TPLUM(M,I-1) = TN(I)
390   35 OIE = TPLUM(M,I-1)-TN(I)
391   IF (OIE.GT. 0.0) GO TO 35
392   MINS = I-1
393   GO TO 36
394   35 CONTINUE

```

```

354 DSS = 0.0
355 MINS = MIN
356 GO TO 42
357 36 IMD = MIN-MINS
358 DO 6 1=1,IMD
359 IF (IMINS+1).GT. MIN) GO TO 67
360 DIFF = IPUM(M,MINSC-1)-TN(MINSC+1)
361 IF 40DIFF.LT. 0.0) GO TO 67
362 MINS = MINSC+1
363 CONTINUE
364 IF (MINS.NE.MIN) GO TO 41
365 DSS = 0.0
366 GO TO 42
367 41 DSS = (MIN-1-MINS)*YS+0.5*YS
368 MINS = MINS-3
369 MINS = MINS-1
370 S = MINS-DSS
371 QCROR(M) = HS*(SAT(M)-TRH(M))
372 QCEIL(M) = HC*(TN(M)-4)-TN(N-5))
373 Q40(M) = HF*(TN(N-4)-TN(3))
374 Q2ST(M) = QCROR(M)-QCEIL(M)-QCRAD(M)
375 Q5P(M) = (C02*(TAC-TN(4))+(FMP(1)*TPAL(M)-COL+C(12)-V(M)*TN(N-
376 X5)))/SHA
377 Q5ST(M) = QCEIL(M)+Q5P(M)
378 IF (V(M).EQ. 0.0) GO TO 211
379 QAC(M) = (C02*(TRH(4)-TAC)+(COL-FMP(1)*TAC-C(12)+VF(M)*TOA(M))*
380 X54)+5.1*VF(M)
381 GO TO 212
382 211 QAC(M) = (C02*(TRH(4)-TAC)+(COL-FMP(1)*TAC-C(12)+VF(M)*TOA(M)-
383 XAC)+5.1*VF(M)+5.1)
384 212 QELINT(M) = HF*(TN(3)-TEMPAC(M))
385 QELST(M) = CG*(T(1)-TEMP)
386 QELST(M) = QCRAD(M)-QELTN(M)-QELOUT(M)+FRL*QL(M)
387 QCL(M) = QACR(M)+QELIN(M)+CLAC
388 QCALL = 0.6729*(TOA(M)-TEMPAC(M))
389 QTOT(M) = 2.8333*QCL(M)+QCALL+7.35
390 IF (V(M).EQ. 0.0) GO TO 213
391 QCHECK(M)=QCROR(M)-QELOUT(M)+(VF(M)*SHA*TOA(M)-TN(N-5))+5.1*VF(
392 X13)+21(M)-QAC(M)-QST(M)-Q5ST(M)-QELST(M)
393 GO TO 214
394 213 QCHECK(M)=QCROR(M)-QELOUT(M)+(VF(M)*SHA*TOA(M)-TAC )+5.1*VF(
395 X1)+21(M)-QAC(M)-QST(M)-Q5ST(M)-QELST(M)
396 214 MINS(M) = MINS
397 IF (CHECK.EQ. 1) QACL(M) = 0.0
398 IF (M.EQ. NON) QACL(M) = QACL(M)+(TEMPAC(M-1)-TAC)*YAC*DA*SHA
399 DO 24 1=1,NIN
400 UMF(M,1) = UFM(1)
401 UMF(M,1) = FM(1)
402 M = M+1
403 IF (M.LT.NTI) GO TO 99
404 WRITE (6,119) OLC,P,VEN,VENS,OLITS,TAC,TPM
405 WRITE (6,105)
406 WRITE (6,106) (M,MINS(M),DS(M),DFAS(M),HFAL(M),BFCHEK(M),VFAL(M),
407 XCHECK(M),TEMPAC(M),TPAL(M),QTOT(M),QCHECK(M), M=1,NTI)
408 WRITE (6,107)
409 WRITE (6,123)
410 WRITE (6,109) (M,(N(M,1), I=1,NIN), M=1,NTI)
411 WRITE (6,110)
412 WRITE (6,108)
413 WRITE (6,109) (M,(RPM(I), I=1,NIN), M=1,NTI)

```

```

448 WRITE (6,111)
449 WRITE (6,108)
450 WRITE (6,109)
451 WRITE (6,112)
452 WRITE (6,108)
453 WRITE (6,109)
454 WRITE (6,113)
455 WRITE (6,114)
456 WRITE (6,115)
457 WRITE (6,116)
458 WRITE (6,117)
459 DO 71 I=1,NTI
460 WRITE (6,118) I,ORDEF(I),QCEIL(I),ORAD(I),ORST(I),QSR(I),QSST(I),
461 XFLIN(I),QFLOUT(I),CFLST(I),QACB(I),QACL(I)
462 STOP
463 END

463 SUBROUTINE GUELM(A,X,M,M1,MS)
C THIS SUBROUTINE PERFORMS GAUSS-JORDAN ELIMINATION NEGLECTING MOST OF THE
C ZEROS IN THE COEF. MATRIX
DIMENSION A(M,M1),X(M)
K1 = M-1
K2 = M-4
K4 = M-6
DO 40 K=1,K1
F = A(K,K)
KP = K+1
A(K,K) = A(K,K)/F
A(K,K+1) = A(K,K+1)/F
IF (K.GT.K4) GO TO 41
A(K,K2) = A(K,K2)/F
41 A(K,M1) = A(K,M1)/F
DO 42 I=1,KP
FP=A(I,K)
IF (K-I) 43,42,43
43 DO 44 J=K,KP
44 A(I,J) = A(I,J)-A(K,J)*FP
IF (K.GT.K4) GO TO 45
A(I,K2) = A(I,K2)-A(K,K2)*FP
45 A(I,M1) = A(I,M1)-A(K,M1)*FP
42 CONTINUE
I = 45
IF (K+1-I) 37,47,47
37 FP = A(I,K)
DO 38 J=K,KP
38 A(I,J) = A(I,J)-A(K,J)*FP
A(I,K2) = A(I,K2)-A(K,K2)*FP
41 A(I,M1) = A(I,M1)-A(K,M1)*FP
47 I = K2
IF (K+1-I) 46,40,40
46 FP = A(I,K)
DO 48 J=K,KP
48 A(I,J) = A(I,J)-A(K,J)*FP
A(I,K2) = A(I,K2)-A(K,K2)*FP
41 A(I,M1) = A(I,M1)-A(K,M1)*FP
40 CONTINUE
K = 4
F = A(K,K)
A(K,K) = A(K,K)/F
A(K,M1) = A(K,M1)/F

```

```

504 DD 49 I=1,K1
505 FP = A(I,K)
506 DO 50 J=K,M1
507 50 A(I,J) = A(I,J)-A(K,J)*FP
508 49 CONTINUE
509 DO 51 I=1,M
510 51 X(I) = A(I,M1)
511 RETURN
512 END

```

SENTRY

Appendix D

Values Used in the Comparison

Most of the values used in the comparison were provided by Dean (2) and a list of them follows.

| | |
|--|--|
| $A_f = 34,000 \text{ ft}^2$ | $k_2 = 0.022 \text{ Btu/hr-ft-}^\circ\text{F}$ |
| $A_w = 9,500 \text{ ft}^2$ | $k_3 = 1.0 \text{ Btu/hr-ft-}^\circ\text{F}$ |
| $c_a = 0.24 \text{ Btu/lbm-}^\circ\text{F}$ | $N = 14$ |
| $c_f = 0.156 \text{ Btu/lbm-}^\circ\text{F}$ | $q_{hl} = 5.02 \text{ Btu/hr-ft}^2$ |
| $c_{st} = 0.115 \text{ Btu/lbm-}^\circ\text{F}$ | $\bar{q}_{int} = 7.35 \text{ Tons of refrigeration}$ |
| $c_l = 0.12 \text{ Btu/lbm-}^\circ\text{F}$ | $Q_{hl} = 853 \text{ Btu/hr}$ |
| $c_2 = 0.157 \text{ Btu/lbm-}^\circ\text{F}$ | $Q_v = 0.206 \text{ cfm/ft}^2$ |
| $c_3 = 0.2 \text{ Btu/lbm-}^\circ\text{F}$ | $R = 7.35 \text{ ft}$ |
| $C_g = 0.148 \text{ Btu/hr-ft}^2\text{-}^\circ\text{F}$ | $\Delta t = 1.0 \text{ hr}$ |
| $d_{lc} = 2.0 \text{ ft}$ | $T_{ac} = 75.0 \text{ }^\circ\text{F}$ |
| $F_{rl} = 0.4$ | $T_g = 55.0 \text{ }^\circ\text{F}$ |
| $F_{st} = 0.01248$ | $T_m = 100.0 \text{ }^\circ\text{F}$ |
| $h_c = 1.08 \text{ or } 1.63 \text{ Btu/hr-ft}^2\text{-}^\circ\text{F}^{**}$ | $U_w = 0.85 \text{ Btu/hr-ft}^2\text{-}^\circ\text{F}$ |
| $h_f = 1.08 \text{ Btu/hr-ft}^2\text{-}^\circ\text{F}$ | $\Delta W = 0.0047 \text{ lbm water/lbm dry air}$ |
| $h_g = 3.0 \text{ Btu/hr-ft}^2\text{-}^\circ\text{F}$ | $y_f = 0.125 \text{ ft}$ |
| $k_a = 0.015 \text{ Btu/hr-ft-}^\circ\text{F}$ | $y_s = 0.3636 \text{ ft}$ |
| $k_f = 0.54 \text{ Btu/hr-ft-}^\circ\text{F}$ | $y_l = 0.005208 \text{ ft}$ |
| $k_l = 360.0 \text{ Btu/hr-ft-}^\circ\text{F}$ | $y_2 = 0.02777 \text{ ft}$ |

$$y_3 = 0.05208 \text{ Ft}$$

** Changes with direction of heat flow, 1.08 downward and 1.63 upward.

$$\alpha = 0.1$$

$$\epsilon_c = 0.5$$

$$\epsilon_f = 0.9$$

$$\rho_a = 0.075 \text{ lbm/ft}^3$$

$$\rho_f = 144.0 \text{ lbm/ft}^3$$

$$\rho_{st} = 490.0 \text{ lbm/ft}^3$$

$$\rho_1 = 489.0 \text{ lbm/ft}^3$$

$$\rho_2 = 10.0 \text{ lbm/ft}^3$$

$$\rho_3 = 95.0 \text{ lbm/ft}^3$$

$$\sigma = 0.1714 \times 10^{-8} \text{ Btu/hr-ft}^2\text{-}^\circ\text{R}^4$$

| Hour | $T_{oa}, ^\circ F$ | $T_{sat}, ^\circ F$ |
|------|--------------------|---------------------|
| 1 | 79 | 72 |
| 2 | 79 | 72 |
| 3 | 78 | 71 |
| 4 | 77 | 70 |
| 5 | 77 | 70 |
| 6 | 77 | 77 |
| 7 | 78 | 88 |
| 8 | 80 | 99 |
| 9 | 83 | 109 |
| 10 | 86 | 118 |
| 11 | 90 | 126 |
| 12 | 93 | 130 |
| 13 | 96 | 132 |
| 14 | 97 | 129 |
| 15 | 98 | 124 |
| 16 | 97 | 116 |
| 17 | 96 | 106 |
| 18 | 94 | 94 |
| 19 | 90 | 83 |
| 20 | 88 | 81 |
| 21 | 86 | 79 |
| 22 | 84 | 77 |
| 23 | 82 | 75 |
| 24 | 80 | 73 |

ACKNOWLEDGEMENTS

The author offers thanks to his major professor, Dr. Robert L. Gorton, who provided guidance and encouragement throughout this investigation. Also, recognition is due to the other members of my graduate advisory committee, Professor John E. Kipp, Professor Harry D. Knostman and Professor David Logan. Mr. Frank, Dean of the Tempmaster Corporation provided the plant data for a comparison with the numerical solution.

Special thanks is given to my parents who provided encouragement throughout my college education.

VITA

Richard A. Beier

Candidate for the Degree of

Master of Science

Thesis: THERMAL STRATIFICATION IN HIGH CEILING FACTORIES

Major Field: Mechanical Engineering

Biographical:

Personal Data: Born in Topeka, Kansas, June 18, 1953, son of Albert P. and Lavina M. Beier.

Education: Attended Hayden High School in Topeka and graduated in May, 1971; received Bachelor of Science degree in Mechanical Engineering from Kansas State University in May, 1975; completed requirements for Master of Science degree December, 1976.

Professional Experience: Employed as a full-time instructor in the School of Engineering Technology at University of Nebraska at Omaha during the 1976-77 academic year.

THERMAL STRATIFICATION IN FACTORIES
WITH HIGH CEILINGS

by

Richard A. Beier

B.S., Kansas State University, 1975

AN ABSTRACT OF A MASTER'S THESIS

submitted in partial fulfillment of the
requirements for the degree

MASTER OF SCIENCE

Department of Mechanical Engineering

KANSAS STATE UNIVERSITY
Manhattan, Kansas

1976

ABSTRACT

In recent years designers of air conditioning systems for factories with high ceilings have used thermal stratification by cooling only the occupied levels. The size and cost of the required systems are significantly less than the systems needed to cool the entire closed space. This study provides a theoretical analysis of the thermal stratification process and some needed design information.

This investigation is limited by considering the light fixtures as the only internal sources which affect the stratification process. The analysis is based on a simplified, physical model in which the level of the light fixtures separates the stratified layer above and the cooled space below. Since the stratified layer also receives heat by convection from the ceiling, the thermal plumes which rise from the lights may not penetrate a stagnant layer of air under the ceiling. It was assumed that exhausting ventilation air through the stratified layer does not alter the motion of the plume or its entrainment of the surrounding air at any level.

An equivalent virtual source for a light fixture was obtained with the same volume and buoyancy flux. Thus, equations previously developed for a thermal plume in a confined region give a steady-state solution to the fluid motion in the stratified layer. However, a transient solution is needed since the cyclic changes in the variables which affect the air conditioning load may not be in phase with each other. The transient energy equations for the roof, floor and stratified layer with appropriate boundary conditions give a concise statement of the problem. These equations are solved numerically by using

implicit finite difference equations and assuming that the fluid motion in the stratified layer remains constant over each time increment. Gauss-Jordan elimination is used to solve the linear system of difference equations. A Fortran computer program using these numerical techniques provides a solution.

The numerical solution was verified by comparing it with data taken at a factory where thermal stratification occurs. The results indicate that convection heat transfer at the ceiling is practically eliminated and only radiation is important. The cooling load can be significantly reduced by exhausting needed ventilation air through the stratified layer and out the roof. Also, it was found that if there is sufficient ceiling height to satisfy the assumptions of the physical model, increasing the ceiling height will not alter the air conditioning load.